02142-502-M

2142-502-M = RL-2042

THE UNIVERSITY OF MICHIGAN

COLLEGE OF ENGINEERING

DEPARTMENT OF ELECTRICAL ENGINEERING

Radiation Laboratory

THE MONOPULSE POINTING ERROR ASSOCIATED WITH A TWO-DIMENSIONAL CONICAL OR OGIVAL RADOME WITH OR WITHOUT A SURROUNDING (WEAK) PLASMA

By

T. B. A. Senior and V. V. Liepa

February 1970

Prepared for

Harry Diamond Laboratories
Microwave Branch, 250
Attn: Dr. Irvin Pollin, AMXDO-RDB
Washington, DC 20438

Ann Arbor, Michigan, 48108
201 East Catherine Street

TABLE OF CONTENTS

I. INTRODUCTION

A problem of continuing practical concern is that of assessing the effect of a radome on the performance of a radar antenna placed within it. If the antenna is required only to radiate a signal and then to detect the time of arrival of an echo from some distant object, the electrical constraints placed upon the radome are very light indeed. Unfortunately, however, such a simple situation is the exception rather than the rule, and more generally the task is to design a radome which will maximize the transmitted power at some frequency (or over a range of frequencies), or will minimize the phase distortions over a range of look angles, and which also satisfies those constraints which are imposed by aerodynamic considerations or by the environment.

An approximate but versatile tool which has been in general use in radome design for many years is geometrical optics, or ray tracing. Taking, for example, the reception problem in which a wave (usually a plane wave) is incident on the outer surface, the incident wave is sampled by means of rays drawn normal to the wave front. Each is traced to the outer surface, and followed as it undergoes refraction at that surface and transmission at the inner one. From a knowledge of the transmission coefficients, which depend on refractive index, polarization and angles of incidence relative to the local normals, and a computation of the electrical distance, an approximate sampling of the field within the radome is obtained. Depending upon the design requirement, the shape and (perhaps) the refractive index of the radome are now adjusted, and to increase the flexibility, multi-layer (sandwich) radomes can be considered.

This is the essence of the theoretical techniques in common use, and though they have proved adequate for many purposes, it should be emphasized that the sampling of the interior field is approximate not only by virtue of the approximations inherent in ray tracing (namely, the assumption that the surfaces all have radii "large" compared with the wavelength), but because the rays reflected at each surface are neglected. On the other hand, to include any reflected rays, many of which would ultimately produce additional ray contributions to the field within the radome, greatly increases the magnitude and complexity of the computation, and was not feasible until the advent of the present generation of high speed, large capacity computers.

The particular problem of interest to us here is one in which the greatest possible accuracy of estimation of the field within the radome is necessary, and in which the inclusion of all possible ray contributions is mandatory. The problem is concerned with the operation of a monopulse radar mounted inside the nose radome of a high speed missile. The radome is either conical or ogival in shape and of single layer construction; its material (fiberglass) is effectively lossless at the C-band frequencies of operation, and for purposes of analysis can be treated as a pure dielectric. The relevant feature of the monopulse system is a gimballed plane containing slots mounted within the radome at a given distance back from the apex. From a comparison of the signals induced in the slots, the monopulse plane is made to take up a position parallel to the effective phase front of the field impinging upon them. Were this field indeed a plane wave, the precise interconnections of the slots through which the comparison is made would be of little relevance inasmuch as any "reasonable" design of monopulse would produce the required alignment. Because of the perturbing effect of the radome, however, the field is not a homogeneous plane wave inside the radome even when the field outside is. The method of comparison of the slot signals will then influence the position taken up by the monopulse plane, and it becomes desirable to record the signals induced in the individual slots. In addition, however, it is convenient to conceive of a simple mode of operation, which is essentially a phase comparison scheme, and which permits a straightforward calculation of the monopulse orientation, and this we shall do.

Since the field inside the radome is a perturbed version of the plane wave incident on its outer surface, the monopulse plane will not in general align itself parallel to the external wavefront. The angle between these two planes is the pointing error of the system, and its determination is one objective of this study. Inasmuch as the system is desired to have, and is presumably designed to have, a pointing error not exceeding 2 milliradians for all polarizations of the incident field, and for all angles from 0^{o} to 55^{o} from axial incidence, the reason why we must include all possible ray contributions, in order to achieve the greatest possible accuracy in the estimation of the field distribution over the monopulse plane, is now apparent. Indeed, it is not without question whether ray tracing can provide this sort of accuracy, but it certainly cannot without taking account of reflections from the inner surfaces of the radome walls, as well as from within the radome layer itself.

Unfortunately, there is a further complication. Because of the speed and altitude at which the missile is required to operate, a plasma layer will be formed just outside the radome wall. In penetrating this layer, the field will suffer a perturbation additional to that produced by the radome itself, and this will in turn produce a change in the pointing error of the monopulse system. Such a change will depend on the nature of the plasma and, hence, upon the altitude, and could negate any attempt (by, for example, shaving or blocking portions of the radome) to minimize the operational pointing error. In consequence, any change in error produced by the plasma is even more serious than the error associated with the bare radome, and the determination of this change is our prime objective.

On setting out to develop and assemble the formulae for three-dimensional ray tracing with even the bare radome, it was at once apparent that the computation of the interior field was an intricate task involving large amounts of time even for a high speed computer. To find, for example, the pointing error for one monopulse system within a specific radome for a wave with a single angle of incidence and polarization, it seemed possible that a running time of as much as one hour on a high speed (IBM 360) computer would be necessary. Subsequent events have shown that this estimate is not unrealistic. It therefore seemed essential to start out with something more simple than the general case, and the two-dimensional analogue of the actual problem was a natural one to choose.

In the two-dimensional problem a conical radome appears as a wedge and an ogive (whose surfaces are arcs of circles) is replaced by one having surfaces which are arcs of circular cylinders. The field is assumed incident in a plane perpendicular to the generators of the surfaces (i.e. in the xy plane), and it is sufficient to consider only the two principal polarization cases in which the electric vector is entirely in the z direction (E-polarization, or TE) or the magnetic vector is so aligned (H-polarization, or TM). Since the entire problem is now two-dimensional and can be expressed in terms of either E_z or H_z, the visualization and details of the analysis are greatly simplified.

The present Memorandum is concerned entirely with this two-dimensional problem. The conception and development of the analyses are described, and the limitations which are imposed by the use of ray tracing are discussed, as are the steps necessary to derive an expression for the monopulse pointing error either with or without a plasma sheath about the radome. Full details of a computer program (in FORTRAN IV) including flow diagram, input data and program listing, are given in the Appendix. Specific results for the pointing error with and without the plasma are presented and discussed. The analogous procedures for the more general three-dimensional problem are described in a companion Memorandum.

Although the two-dimensional radome is, of course, a mathematical idealization, it should be emphasized that we do not consider the case treated here as one having academic interest only. The practical purpose for our study is to see whether it is realistic to expect a maximum pointing error of 2 milliradians for a wide range of aspect angles, with or without a (weak) plasma sheath. The pointing error arises because of the field distortion produced by radome reflections. A three-dimensional geometry will produce more reflections than does the two dimensional, and perturb the wave front in three directions rather than two. It is therefore only natural to expect that the results for the two-dimensional geometry will constitute a lower bound on the pointing errors that will occur in the three-dimensional case. As will be shown, the errors found using the two-dimensional geometry in general exceed the 2 milliradian requirement.

II. RAY OPTICS FOR A DIELECTRIC SLAB

It is a straightforward but instructive problem to examine the transmission of a plane electromagnetic wave through a homogeneous and isotropic dielectric slab. Although this topic is treated in many electromagnetic theory texts and in almost all books devoted to optics, the results and their interpretation play such a vital role in the treatment of the radome problem that a brief discussion is desirable.

Consider a plane dielectric slab of thickness d and infinite extent occupying $a \leq y \leq a + d$, where (x, y, z) are rectangular Cartesian coordinates. It is sufficient to take the permeability of the dielectric to be the same as that of free space, i.e. $\mu = \mu_0$, but the permittivity ϵ differs from ϵ_0, and we define the refractive index n of the dielectric relative to free space to be $n = \sqrt{\epsilon/\epsilon_0}$. The regions above and below the slab are occupied by free space.

A plane electromagnetic wave is incident on the lower face of the slab. We treat first the case in which the wave is H-polarized, i.e. TM, and write the incident field as

$$\underline{H}^i = \hat{z}\, e^{ik(x \sin\alpha + y\cos\alpha)}$$
$$\underline{E}^i = -Z_0 (\hat{x}\cos\alpha - \hat{y}\sin\alpha)\, e^{ik(x\sin\alpha + y\cos\alpha)} \tag{1}$$

where $Z_0 = \sqrt{\mu_0/\epsilon_0}$ is the characteristic impedance of free space, and a time factor $e^{-i\omega t}$ has been suppressed. As evident* from Fig. 1, α is the angle which the propagation vector makes with the normal to the slab.

To find the field transmitted through the slab, we postulate the following field expressions:

---
*Figures are placed at the end of each section.

$y \leq a$:

$$\underline{H} = \hat{z}\left\{e^{ik(x\sin\alpha + y\cos\alpha)} + Ae^{ik(x\sin\alpha - y\cos\alpha)}\right\},$$

$$\underline{E} = -Z_0\left[\hat{x}\ \cos\alpha\left\{e^{ik(x\sin\alpha + y\cos\alpha)} - Ae^{ik(x\sin\alpha - y\cos\alpha)}\right\}\right. \qquad (2)$$

$$\left. -\hat{y}\sin\alpha\left\{e^{ik(x\sin\alpha + y\cos\alpha)} + Ae^{ik(x\sin\alpha - y\cos\alpha)}\right\}\right];$$

$a \leq y \leq a+d$:

$$\underline{H} = \hat{z}\left\{Be^{ink(x\sin\beta + y\cos\beta)} + Ce^{ink(x\sin\beta - y\cos\beta)}\right\},$$

$$\underline{E} = -\frac{Z_0}{n}\left[\hat{x}\cos\beta\left\{Be^{ink(x\sin\beta + y\cos\beta)} - Ce^{ink(x\sin\beta - y\cos\beta)}\right\}\right. \qquad (3)$$

$$\left. -\hat{y}\cos\beta\left\{Be^{ink(x\sin\beta + y\cos\beta)} + Ce^{ink(x\sin\beta - y\cos\beta)}\right\}\right];$$

$a + d \leq y$:

$$\underline{H} = \hat{z}\,De^{ik(x\sin\alpha + y\cos\alpha)},$$

$$\underline{E} = -Z_0\ (\hat{x}\cos\alpha - \hat{y}\sin\alpha)\ De^{ik(x\sin\alpha + y\cos\alpha)}\ . \qquad (4)$$

The unknown coefficients, A, B, C and D can be determined from the boundary conditions at the two faces of the slab, which conditions require that $\underline{H}\cdot\hat{z}$ and $\underline{E}\cdot\hat{x}$ be continuous there. Applying these conditions, we obtain

$$e^{ika\cos\alpha} + Ae^{-ika\cos\alpha} = Be^{inka\cos\beta} + Ce^{-inka\cos\beta},$$

$$e^{ika\cos\alpha} - Ae^{-ika\cos\alpha} = \frac{1}{\Gamma}\left\{Be^{inka\cos\beta} - Ce^{-inka\cos\beta}\right\},$$

$$De^{ik(a+d)\cos\alpha} = Be^{ink(a+d)\cos\beta} + Ce^{-ink(a+d)\cos\beta},$$

$$De^{ik(a+d)\cos\alpha} = \frac{1}{\Gamma}\left\{Be^{ink(a+d)\cos\beta} - Ce^{-ink(a+d)\cos\beta}\right\},$$

where

$$\Gamma = \frac{n \cos\alpha}{\cos\beta} \tag{5}$$

with

$$\sin\beta = \frac{\sin\alpha}{n} \qquad \text{(Snell's law)}, \tag{6}$$

and hence

$$C = \frac{1}{2}(1-\Gamma)\, D e^{ik(a+d)(\cos\alpha + n\cos\beta)} ,$$

$$B = \frac{1}{2}(1+\Gamma)\, D e^{ik(a+d)(\cos\alpha - n\cos\beta)} ,$$

$$A = -\frac{i}{2}\left(\Gamma - \frac{1}{\Gamma}\right) D \sin(nkd\cos\beta) e^{ik(2a+d)\cos\alpha} ,$$

with

$$D = \frac{4\Gamma e^{ikd(n\cos\beta - \cos\alpha)}}{(\Gamma+1)^2 - (\Gamma-1)^2 e^{2inkd\cos\beta}} . \tag{7}$$

D represents the transmission coefficient of the slab and is the quantity of most interest to us. Its exact expression is given in Eq. (7), but for future purposes an alternative representation is more convenient, viz.

$$D = \sum_{m=1}^{\infty} D_m , \tag{8}$$

where

$$D_m = \frac{4\Gamma}{(\Gamma+1)^2} e^{ikd(n\cos\beta - \cos\alpha)} \left(\frac{\Gamma-1}{\Gamma+1}\right)^{2(m-1)} e^{2i(m-1)nkd\cos\beta} . \tag{9}$$

Each term D_m in (8) can be associated with a partial transmitted field

$$\begin{aligned} \underline{H}^{(m)} &= \hat{z} D_m e^{ik(x\sin\alpha + y\cos\alpha)} , \\ \underline{E}^{(m)} &= -Z_o (\hat{x}\cos\alpha - \hat{y}\sin\alpha) D_m e^{ik(x\sin\alpha + y\cos\alpha)} , \end{aligned} \tag{10}$$

and to appreciate the origin of this field, consider for the moment the simpler problem shown in Fig. 2. The dielectric now occupies the entire half-space $y \geq a$, and if the incident field is again that given by the Eqs. (1), the reflection and transmission coefficients are, respectively,

$$R_{12} = \frac{\Gamma - 1}{\Gamma + 1} e^{2ika \sin\alpha} ,$$

$$T_{12} = \frac{2\Gamma}{\Gamma + 1} e^{ika(\cos\alpha - n\cos\beta)} , \tag{11}$$

as shown in many standard texts. The first suffix refers to the medium in which the wave is incident (1 denotes free space) and the second refers to the medium at which it is reflected or into which it is transmitted (2 denotes the dielectric). Alternatively, if the dielectric occupies the half-space $y \leq a + d$ (see Fig. 3) so that the interface is illuminated by a wave propagating in the denser medium and of the form given by the leading terms in the Eqs. (3), the reflection and transmission coefficients are

$$R_{21} = -\frac{\Gamma - 1}{\Gamma + 1} e^{2ink(a+d)\cos\beta} ,$$

$$T_{21} = \frac{2}{\Gamma + 1} e^{ik(a+d)(n\cos\beta - \cos\alpha)} , \tag{12}$$

where Γ and β are again as defined by Eqs. (5) and (6) respectively.

With the aid of (11) and (12), the interpretation of the partial fields $\underline{H}^{(m)}$, $\underline{E}^{(m)}$ is now obvious. As evident from the moduli and phases of the coefficients D_m, m=1, 2, 3,... (see Eq. 9), $\underline{H}^{(1)}$, $\underline{E}^{(1)}$ is the field produced by refraction at the lower interface of the slab as though the upper interface were not present, followed by a refraction of this wave at the upper interface as though the lower interface were not present. Indeed,

$$D_1 = T_{12} T_{21} .$$

Likewise, $\underline{H}^{(2)}$, $\underline{E}^{(2)}$ arises from a refraction at the lower interface, reflection at the upper interface, reflection at the lower interface and a refraction at the upper interface, so that

$$|D_2| = |T_{12}R_{21}R_{21}T_{21}|$$

with the phase of D_2 being that appropriate to the zig-zag path; and so on. We can therefore build up the exact field transmitted through the slab by considering each interface separately, and by superposing the partial fields resulting from all possible bounces within the layer. Each partial field is such that the boundary conditions at the isolated interfaces are exactly satisfied, but it is only through the superposition of all these fields that the boundary conditions at both interfaces are jointly satisfied regardless of d, and of the absence of losses within the dielectric.

If, instead of an H-polarized (or TM) wave, the field incident on the slab is an E-polarized (or TE) plane wave, such that

$$\begin{aligned} \underline{E}^i &= \hat{z}\, e^{ik(x \sin\alpha + y \cos\alpha)}, \\ \underline{H}^i &= Y_0\, (\hat{x}\cos\alpha - \hat{y}\sin\alpha)\; e^{ik(x\sin\alpha + y\cos\alpha)} \end{aligned} \tag{13}$$

with $Y_0 = {}^1/Z_0$, the analysis goes through just as before with the sole difference that n is now replaced by ${}^1/n$. Hence

$$\Gamma \rightarrow \frac{\cos\alpha}{n\cos\beta} = \Gamma' , \tag{14}$$

and the reflection and transmission coefficients (based, of course, on $\underline{E}$) for single interfaces are as given in Eqs. (11) and (12) with n replaced by ${}^1/n$ and therefore Γ replaced by Γ'.

Although the above description has been phrased in terms of partial (plane wave) fields, it is obvious that the picture that has evolved is identical to that which is provided by geometrical optics, i.e. ray theory. Starting from any point in the region below the slab, we trace the ray through this point and perpendicular to the incident wave front (i.e. in the direction of the propagation vector of the incident field) until the ray meets the lower interface of the slab. Here it undergoes reflection and refraction. The refracted ray now makes an angle β with the normal to the slab and proceeds with the decreased velocity c/n until it hits the upper interface, where reflection and refraction takes place. The refracted ray provides a direct sample of the field above the slab. The reflected ray is followed back to the lower interface, thence to the upper interface, to provide another sampling of the field in $y \geq a + d$; and so on. This one single incident ray therefore provides an infinite sequence of discrete samplings of the field in $y \geq a + d$. Moving now to an adjacent point on the same incident wavefront, we repeat the process to provide yet another sequence of samples, but because of the planar nature of the geometry, it is apparent that the second sequence differs from the first only by a linear shift. It is this fact which permitted a discussion in terms of partial fields, thereby obviating the need for sampling the incoming field. For other than a planar geometry the partial fields would not be plane waves and could not be easily obtained. We then have no alternative but to resort to ray theory and to sample the incoming wavefront over that portion that produces a significant contribution to the field beyond the dielectric in the region of space of interest to us. Clearly, the samples must be sufficiently close ($\ll \lambda$) for the rays to be reasonably dense throughout this spatial region, and in particular, if there are several different categories of rays, we must ensure that several rays of each category are included.

Nevertheless, it should go without saying that the solution obtained in this more general case is only approximate no matter how many reflections within the layer are included, and no matter how closely the incident wavefront is sampled, but if the lateral dimensions (including radii of curvature) of the interfaces are large compared with the wavelength, and if all caustic or focussing effects (where an infinity of rays come together) can be ignored, the solution should reproduce the dominant features of the true transmitted field, and be accurate enough for most practical purposes. These conditions would appear to be fulfilled in the radome problem to which this technique will be applied.

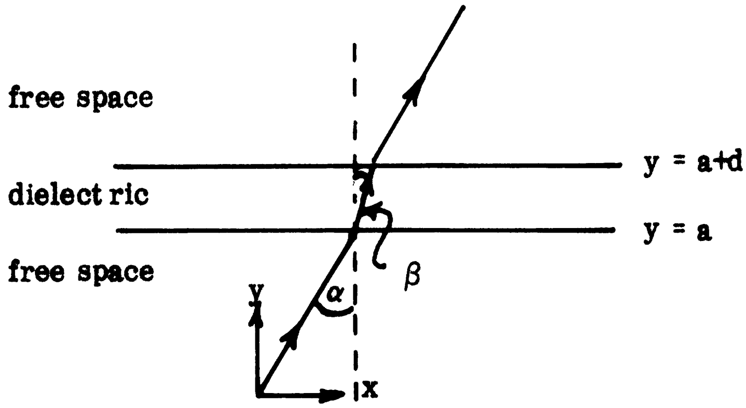

Fig. 1: Slab Geometry

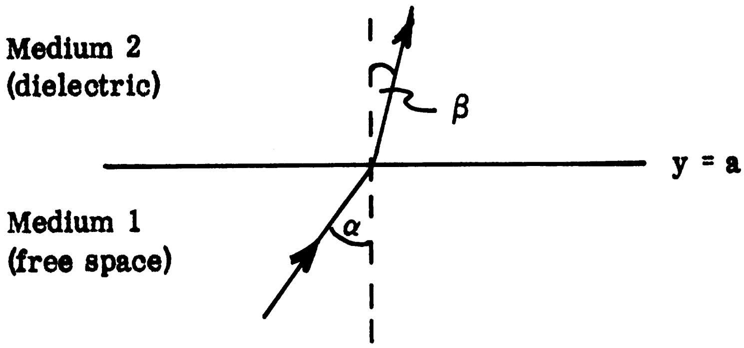

Fig. 2: Geometry for Single Interface (a) .

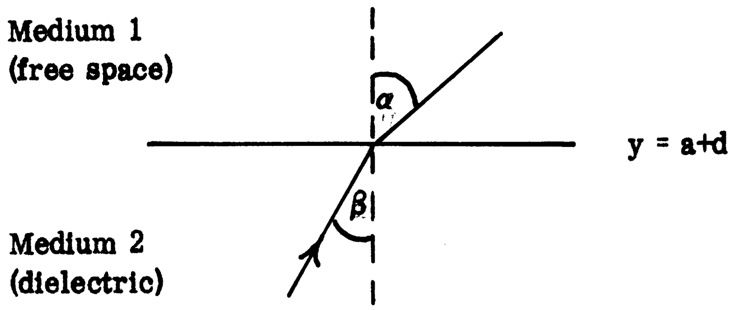

Fig. 3: Geometry for Single Interface (b) .

III APPLICATION TO A BARE RADOME

Consider a two dimensional radome symmetrical with respect to the plane y = 0 of a rectangular Cartesian coordinate system (x, y, z) and whose outer and inner surfaces have generators parallel to the z axis. A plane electromagnetic wave is assumed incident on the outer surface of the radome, and by taking its direction of propagation to be perpendicular to the z-axis, the entire problem becomes two dimensional. It is then sufficient to confine attention to the plane z = 0, and each surface of the radome can be defined by an equation of the form y = f (x) .

Two particular* radome configurations are considered, namely, ogival and conical. In either instance it is assumed that the outer and inner surfaces are both ogival or both conical, and whilst this still permits the radome thickness to be non-uniform, it will be appreciated that the type of thickness variation that can be considered is quite restricted.

For computational purposes it is convenient to choose the origin of the coordinates at a small but non-zero distance ℓ to the left of the 'nose' of the radome (see Fig. 4). In the ogival case, the outer surface can then be defined by the equation

$$y_{outer} = \pm \left(\sqrt{A^2+B^2-(x-C)^2} - A \right) \tag{15}$$

with the upper (lower) sign referring to the upper (lower) surface of the radome, and where A, B and C are positive real numerical constants in terms of which the maximum diameter of the radome is

$$2 \left(\sqrt{A^2+B^2} - A \right)$$

occurring at x = C, the radius of the curvature is R, where

$$R = \sqrt{A^2 + B^2} \quad ,$$

---

*The extension to any radome configuration that can be analytically defined is entirely trivial.

and $\ell = C - B$.

The overall length of the radome is 2B, but in practice interest is confined to that portion of the interior extending to at most the position of the maximum diameter, i.e. to $x \leq C$. The inner surface of the radome is defined in a similar manner.

For the conical case, the definitions of the radome surfaces are more straightforward, and for the outer surface we have

$$y_{outer} = \pm a\,(x - \ell)\,, \qquad (x \geq \ell) \tag{16}$$

where the upper (lower) sign again refers to the upper (lower) surface of the radome. The inner surface is defined in a similar manner, but with a different value for ℓ .

Regardless of the configuration, the radome is assumed to be of single layer construction and formed from a material which can be treated as a homogeneous, isotropic and lossless dielectric whose permeability is the same as that of free space. The electromagnetic properties of the material can therefore be represented by the (real) refractive index n . A typical value is n = 2.5 appropriate to fiberglass at a frequency in the GHz range.

Before detailing the various steps in the ray tracing procedure, a few words about the overall objective of the program are desirable. Although ray tracing could be used to determine the field characteristics anywhere within the radome, the particular objective is to assess the performance of a (receiving) monopulse system. The monopulse plane pivots about an axis parallel to the z axis and located at a point $x = D \leq C$, its orientation being determined from a comparison of the signals induced in a number of slots located in its plane. If the field inside the radome were indeed a plane wave propagating in the same direction as the external field incident on the radome, the monopulse would align its plane parallel to the external wave front. Because of the existence of the radome, however, the field inside differs from that outside, and the monopulse can be expected to take up a position which is not quite parallel to the external wavefront, but differs by some small angle ϵ, which is then the pointing error of the system. On the assumption that both the radome and monopulse systems are well designed, ϵ will be of the order of a few milliradians or less, and it is then sufficient to assume that the monopulse plane is actually parallel to the external wavefront, and to deduce a pointing error in the manner described in Section IV. Only in the event that the error so obtained was measured in several tens of milliradians would it be necessary to re-align the plane over which the field distribution was being sought. No such case has been found, and we can therefore state the intent of the ray tracing as the determination of the field distribution in amplitude and phase over a plane parallel to the incident wavefront and centered on a line parallel to the z axis at a distance $D - \ell$ back from the front of the radome.

Consider a plane TE or TM wave incident on the radome at an angle* β to the plane $y = 0$, i.e. the x axis, as shown in Fig. 5, and take as basis the zero phase wavefront passing through the origin. Choose a point (x_0, y_0) on this wavefront (clearly, $x_0 = -y_0 \tan \beta$), and follow the ray through this point (and normal to the wavefront) until it strikes the radome. Obviously this will be the outer surface, and we can ensure that it is also the lower surface by taking y_0 sufficiently large and negative. Find the point of intersection (x_1, y_1) and record the distance $d_{01} = \left\{(x_1-x_0)^2+(y_1-y_0)^2\right\}^{1/2}$. Compute the direction of the outward normal to the surface at this point and hence determine α, the angle which the ray makes with the normal. The angle which the refracted ray makes with the normal can now be found from Snell's law (Eq. 6) and the amplitude of the ray is T_{12}. Follow this ray until it strikes the inner surface of the radome and compute the point (x_2, y_2) of intersection. Record the 'optical' distance $n\, d_{21} = n \left\{(x_2-x_1)^2 + (y_2-y_1)^2\right\}^{1/2}$ and add to d_{01}. Compute the direction of the normal to the surface at (x_2, y_2), thereby finding the direction which the ray makes with the normal, and allowing the

*This is the angle between the direction of propagation and the x axis.

determination of the direction and strength $T_{12}T_{21}$ of the transmitted ray. Follow this ray until it (i) strikes the monopulse plate at a point (x_p, y_p), in which case the distance $d_{2p} = \left\{ (x_p - x_2)^2 + (y_p - y_p)^2 \right\}^{1/2}$ is computed and added to $d_{o1} + nd_{21}$, and the result recorded along with the strength $T_{12}T_{21}$ of the ray and the direction which it makes with the horizontal; or (ii) passes beyond the monopulse plate between the extremities of this plate and the inner radome surface, in which case the ray contribution is ignored, and attention reverts to the previous intercept of the ray with an inner radome surface; or (iii) the ray strikes an inner (upper) radome surface. In this event the point of intercept (x_3, y_3) and the normal direction are computed, along with the accumulated (optical) ray distance to this point. The direction and amplitude $T_{12}T_{21}R_{12}$ of the reflected ray are found, and the ray followed until it strikes the monopulse plate (and is recorded), or passes beyond the plate (and is ignored), or strikes the radome again. If it does strike the radome, the process is continued, but ultimately the amplitude of such a ray will fall below a pre-set level, and can then be ignored on this account.

Having followed a 'dominant' ray to a conclusion, attention is transferred to the previous intercept of this ray with a radome surface, and the reflected or refracted ray that was omitted is now considered, and this also followed to a conclusion. But in the course of its path, this ray may also have spawned further rays by reflection and refraction, and these too must be picked up and traced through to a conclusion; and so on, arriving ultimately at the stage at which all significant contributions generated by the original ray through the point (x_o, y_o) have been considered. We now return to the incident wave front and step a distance Δ along it, where Δ is some pre-set value $<< \lambda$. The above process is then repeated with the ray originating at the point

$$\left(-(y_o + \Delta \cos \beta) \tan \beta,\ y_o + \Delta \cos \beta \right)$$

and so on until, with further stepping, no rays can be found to intercept the monopulse plate.

The procedure should now be apparent. Each individual computation is rather simple, requiring only the calculation of an intercept point, a normal, a distance and an angle, and from these, Γ (or Γ') and transmission and reflection coefficients; but because of the considerable number of such computations entailed in following one ray through the radome and on to the monopulse plate (one ray may produce many tens of significant contributions to the monopulse field), the process would be extremely tedious to carry out by hand. Nevertheless, it is well suited to a digital computer, and the only complicated aspect of the programming is the ordering of the sequence in which the ray contributions are computed to ensure that no significant rays are omitted.

For each polarization (TM or TE) there is just one form of reflection coefficient that must be computed, but two forms of transmission coefficient. Thus, for a TM wave, we have*

$$R_{12} = - R_{21} = \frac{\Gamma-1}{\Gamma+1} , \qquad (17)$$

$$T_{12} = \frac{2\Gamma}{\Gamma+1} , \qquad (18)$$

$$T_{21} = \frac{2}{\Gamma+1} , \qquad (19)$$

where

$$\Gamma = \frac{n \cos\alpha}{\cos\beta} , \qquad (20)$$

with $\sin\beta = \frac{\sin\alpha}{n}$, and the notation is as shown in Figs. 2 and 3. Since $n > 1$ (typically, 2.5), any (real) α gives rise to a real value of β, and Γ is a monotonically decreasing function of α, ranging from a maximum of n for $\alpha = 0$, through unity for $\alpha = \tan^{-1} n$ (Brewster angle), to zero for $\alpha = \pi/2$. As a consequence of this, R_{12} is also a monotonically decreasing function for $0 \leq \alpha \leq \tan^{-1} n$, and is quite small for most angles of interest to us, but for increasing $\alpha > \tan^{-1} n$, $-R_{12}$ increases rapidly to unity. The situation

---

*The phase factors appearing in Eqs. (11) and (12) are here omitted since they are picked up in the computation of the (normalized) distances along rays.

is, however, somewhat different as a function of β^*, i.e. if the ray starts within the denser medium. A real β gives rise to a real α only if $|\sin\beta| \leq \frac{1}{n}$, and as a function β, Γ varies from n for $\beta = 0$ down to zero for $\beta = \sin^{-1}\frac{1}{n}$. For larger β, Γ is pure imaginary and total internal reflection occurs.

For an incident TE wave,

$$R_{12} = -R_{21} = \frac{\Gamma' - 1}{\Gamma' + 1} , \tag{21}$$

$$T_{12} = \frac{2\Gamma'}{\Gamma' + 1} , \tag{22}$$

$$T_{21} = \frac{2}{\Gamma' + 1} , \tag{23}$$

where

$$\Gamma' = \frac{\cos\alpha}{n\cos\beta} . \tag{24}$$

Since $\Gamma' = \Gamma/n^2$, Γ' is a monotonically decreasing function of α varying from a maximum of $1/n$ for $\alpha = 0$ to 0 for $\alpha = \pi/2$. Since it is always less than unity, R_{21} is a monotonically increasing function, and for most angles of interest to us, the reflection coefficient for TE waves is substantially greater than for TM waves. This implies a larger number of significant ray contributions in the former case.

There are two final comments that should be made, one pertaining to both radomes and the other to the ogival one only. We have noted that the determination of a ray path requires the calculation (or knowledge) of the direction of the local normals to the radome surfaces. With both radomes, the normal is undefined at the very apices of the inner and outer surfaces, and to avoid difficulty in this regard, any ray which hits these points is automatically terminated. This is equivalent to assuming the radome to have infinitesimal opaque 'plugs' here. The second comment applies only to the ogival radome whose surfaces

---

* β and α are here the angles used in Section II.

in the xy plane are curved. Because of this curvature and, in consequence, the slight difference in the directions of the normals at different distances from the apex, it is possible that a ray striking the outer surface at an angle very close to grazing may, on reaching the inner surface, find itself within the critical angle and be entirely reflected. The reflection coefficient is then complex and would require a modification to the program. It is fortunate, however, that for convex surfaces (as we are dealing with) such a ray can never provide a non-attenuated ray contribution within the radome: no matter how many more reflections it undergoes within the layer, it will continue to be critically reflected at the inner radome surface. Any ray that is critically reflected can therefore be abandoned.

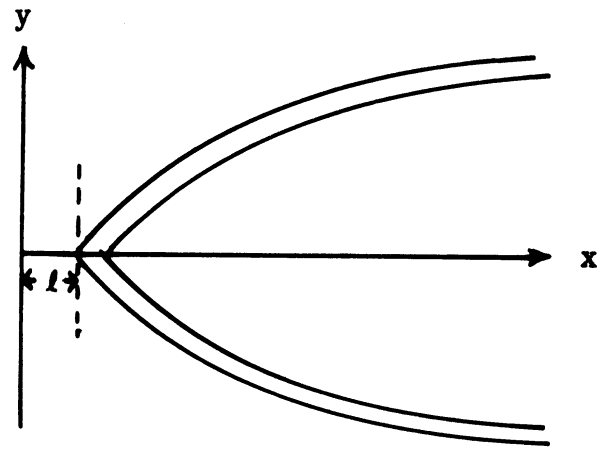

Fig. 4 : Coordinate System.

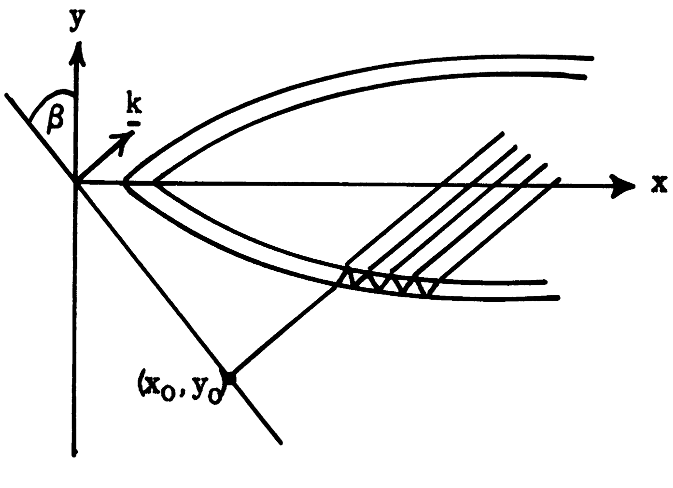

Fig. 5 : Ray Tracing .

IV MONOPULSE RESPONSE

The end result of the ray tracing procedure described in the previous section and implemented in Section VI is a sampling of the field distribution over a monopulse plane aligned parallel to the external wave front and centered at a distance D - ℓ back from the front of the radome. Each sample is an individual ray contribution and consists of an amplitude (which may be positive or negative), accumulated (optical) ray distance (in inches) and a direction of arrival measured with respect to the x axis. The distance can be converted to a phase by multiplying by $k = 2\pi/\lambda$, where λ is the wavelength (in inches), and we can express the direction of arrival as an angle ϕ measured from the normal to the monopulse plane by subtracting β. Each sample now takes the form

$$A_n, \qquad \psi_n, \qquad \phi_n$$

implying a contribution

$$A_n e^{i\psi_n}, \quad \angle\phi_n ,$$

where A_n is a real (positive or negative) amplitude and ψ_n is a phase.

If the radome were not present, each sampling of the incident wavefront would provide a single sample in the monopulse plane. The spatial distributions of the two samplings would then be the same and we should have

$$A_n = 1, \qquad \psi_n = \text{constant}, \qquad \phi_n = 0 ,$$

appropriate to a plane wave incident on the monopulse plane. In this case, the signal in the difference channel of the monopulse would be zero for its plane oriented as chosen: the chosen plane would therefore be the actual monopulse plane, and the pointing error would be zero.

Because of the radome, however, the field inside will not be identical to that outside and will not, in fact, be a plane wave. Each ray drawn from the incident wavefront will generate an infinity of rays within the radome, a finite number of which will intercept the monopulse plate in a spatially non-uniform pattern. The composite of all such rays obtained by sampling the wavefront at a uniformly-spaced set of points constitutes our sampling of the field distribution over the monopulse plane from which we have to deduce the monopulse response. It is to be expected that the difference channel of the monopulse system will contain a non-zero signal which would produce a re-alignment of the monopulse plane through a small angle ϵ which is then the (angular) pointing error. The determination of ϵ is our objective.

Since the monopulse is required to operate only on reception, it is sufficient to regard it merely as a 'split beam' system in which the fields induced in identical slots symmetrically placed on the two halves of the monopulse plane are compared, and from the difference signal, the effective direction of the excitation field is deduced. In the simplest version of this system, we have just two slots, one on either side of the center of the monopulse plane, as shown in Fig. 6. With ξ a running variable on the surface of the monopulse plate in the xy plane, let $\xi = \pm \xi_1$ be the coordinates of the centers of the two slots, and let 2d be the width of each slot. The upper slot therefore extends from $\xi = \xi_1 - d$ to $\xi_1 + d$ and the lower from $\xi = -\xi_1 + d$ to $-\xi_1 - d$, and only if a ray strikes the monopulse plate inside one of these apertures can it contribute to the signal induced in that slot.

The corollary to this last statement is that a ray which strikes the monopulse plane outside a slot does not contribute, and this is certainly reasonable as regards any immediate contribution. But if the monopulse plate outside the slots is metallic; or, more generally, if it is not absorbing to an extent which is complete for all practical purposes, a ray striking this portion of the plate will be reflected and will thereby generate a whole series of new ray families, some of whose members may return to the monopulse plate and strike it within the slots. The directions of these further rays will bear no direct relation to the direction of the wave normal (or rays) of the incident field outside the radome, and will serve, in general, to increase the pointing error of the system. Since we are concerned to keep the pointing error as small as possible, it is desirable to suppress these rays, and this we can do by the mere process of placing a layer of appropriate absorbing material on the monopulse plate outside the slots. At the frequency of interest the absorber could be quite thin, and would not appear to have any deleterious effect on the performance of the system: indeed, it could be advantageous in decreasing the far side lobe levels of the individual slots. For these reasons, we shall neglect any contributions from rays which do not strike a slot, and will presume that the monopulse plate is so treated as to suppress any reflections if these would otherwise produce more unwanted ray contributions of significant magnitude within the slots. We note that such suppression would probably occur naturally if the monopulse consisted of two (or more) horn antennas rather than slots in a base plate.

Although all rays that strike a slot contribute to the signal induced, it would be unreasonable to assume that the magnitudes are the same regardless of the directions at which the rays impinge. In order to take this effect into account, a polar diagram is associated with each slot, and for convenience this is taken to be

$$P(\phi) = \frac{\sin(2kd\sin\phi)}{2kd\sin\phi} \quad , \tag{25}$$

where ϕ is measured from the normal to the plane of the slot (see Fig. 6). Although such a factor is generally used for plane wave incidence, it will be assumed that this same factor obtains for the non-planar, inhomogeneous field that is actually present, implying a reduction in the magnitude of each ray contribution with increasing angle from the normal; and though the actual factor appropriate to a particular practical system may differ somewhat from (25), the differences are unlikely to be significant for our purposes. Were it necessary to do so, any function capable of analytic representation could be used in place of (25) in the digital program.

Combining Eq. (25) with the form of each ray contribution previously arrived at, the signal induced in the slot centered on $\xi = \xi_1$ can be written as

$$V_+ e^{i\Psi_+} = \sum_n A_n P(\phi_n) e^{i\psi_n} \quad , \tag{26}$$

where the summation extends over those rays which strike the aperture. It will be observed that the angle of arrival of each ray affects the output of the slot only through the polar diagram factor $P(\phi)$. Likewise, for the slot centered on $\xi = -\xi_1$, the output is

$$V_- e^{i\Psi_-} = \sum_n A_n P(\phi_n) e^{i\psi_n} \quad , \tag{27}$$

and from a comparison of these outputs the pointing error of the monopulse must be deduced.

Since the field within the radome is at least approximately a plane wave, V_+ and V_- will be very close in magnitude, and the most natural method of comparison is based on phase, i.e. Ψ_+ and Ψ_- , alone. We also note that this pseudo plane wave is incident in a direction which is almost normal to the plane of the slots, and in expectation that the average direction of propagation makes only a small angle ϵ with the normal to the monopulse plate, which angle is the pointing error of the system, we can now proceed as follows.

If a plane wave travelling in a direction $\phi - \epsilon$ (see Fig.7) with respect to the positive x axis were incident on the monopulse, the phase of the signal in the upper slot with respect to the pivot point would take the form

$$e^{-ik \xi \sin \epsilon}$$

and for sufficiently small ϵ, the dominant effect of this aperture distribution on the radiation polar diagram is to displace the effective phase center a distance $\xi_1 \sin \epsilon$ behind the slot. For the lower slot the phase center is brought a distance ξ_1 sin ϵ forward, and from a comparison of Eqs. (26) and (27) it now follows that

$$2k\xi_1 \sin\epsilon = \Psi_+ - \Psi_- \quad , \tag{28}$$

implying a pointing error

$$\epsilon = \sin^{-1}\left\{\frac{\lambda}{4\pi\xi_1}(\Psi_+ - \Psi_-)\right\} \quad . \tag{29}$$

The above description has been phrased in terms of two slots, but a monopulse system will in general have more. The extension to any (even) number 2M of slots is quite straightforward, and the computer program (see Appendix) has been written to permit up to 6 equal-width slots symmetrically placed with respect to the middle of the monopulse plane. The resulting expression for the pointing error now depends on the manner in which the outputs from the various slots are combined. If the centers of the slots are located at $\xi = \pm\xi_1, \pm\xi_2, \pm\xi_3, \ldots$, and the corresponding outputs are

$$V_\pm^{(1)} e^{i\Psi_\pm^{(1)}} \, , \quad V_\pm^{(2)} e^{i\Psi_\pm^{(2)}} \, , \quad V_\pm^{(3)} e^{i\Psi_\pm^{(3)}} \, , \ldots \, ,$$

one approach is to combine all the outputs from the slots on the upper half of the plane to give

$$\bar{V}_+ e^{i\bar{\Psi}_+} = \sum_m W_m V_+^{(m)} e^{i\Psi_+^{(m)}} \quad ,$$

and similarly combine the outputs from the lower slots, giving

$$\bar{V}_- e^{i\bar{\Psi}_-} = \sum_m W_m V_-^{(m)} e^{i\Psi_-^{(m)}} \quad ,$$

where the W_m are the appropriate (amplitude) weighting factors of the slots. The pointing error ϵ can then be obtained from the expression

$$\epsilon = \sin^{-1}\left\{\frac{\lambda}{4\pi\bar{\xi}}\left(\bar{\psi}_{+} - \bar{\psi}_{-}\right)\right\} , \tag{30}$$

where $\bar{\xi}$ is a 'mean' position of the combined slots, given by

$$\bar{\xi} = \frac{\sum_{m} W_m \xi_m}{\sum_{m} W_m} . \tag{31}$$

Although the above procedure is the one that was actually adopted, it should be noted that it is by no means the only way of finding an expression for the pointing error. We could, for example, compare the outputs of corresponding slots, and then average the individual pointing errors to produce a value for ϵ , viz.

$$\epsilon = \frac{1}{M} \sum_{m=1}^{M} \sin^{-1}\left\{\frac{\lambda}{4\pi\xi_m}\left(\bar{\psi}_{+}^{(m)} - \bar{\psi}_{-}^{(m)}\right)\right\},$$

which is approximately

$$\epsilon \simeq \sin^{-1}\left\{\frac{1}{M} \sum_{m=1}^{M} \frac{\lambda}{4\pi\xi_m}\left(\bar{\psi}_{+}^{(m)} - \bar{\psi}_{-}^{(m)}\right)\right\} \tag{32}$$

on the assumption that each individual error is small. In this form, ϵ is independent of any amplitude weighting applied to the slots.

When the original approach was programmed, it was found that a slight displacement of the initial (and, hence, all subsequent) point(s) at which the incident phase front was sampled led to a small but detectable change in ϵ . Such a displacement produces, in turn, a shift in the position at which the rays hit the monopulse plate , and when this causes a dominant ray to strike just outside (instead of just inside) the slot, a discontinuity in the induced signal results. With the sampling frequency that was used, the maximum discontinuity observed was no more than (about) 10 percent, and was not therefore a severe problem. Nevertheless, it seemed desirable to seek a reduction in the discontinuity , particularly because of our ultimate aim of comparing pointing errors with and without a plasma present.

An obvious way of reducing the effect is to decrease significantly the distance between successive sampling points, thereby decreasing the relative weight attached to any one ray contribution. This would, however, markedly increase the length of an already-long computation, and since the main objective was to provide a smooth transition as any one ray traverses the boundary of a slot, it is sufficient to assign an amplitude taper to each slot. Each ray contribution is then weighted according to the position at which the ray strikes the slot, the weighting varying from unity at the center of the slot to zero at the boundary. The same taper was applied to each slot, and the particular taper assumed was

$$T(\xi) = \cos^2\left\{\frac{\pi}{2d}(\xi-\xi_m)\right\} \quad , \tag{33}$$

where ξ is the position at which the ray impinges and ξ_m is the coordinate of the midpoint of the (m th) slot. Each term in the summands in Eqs. (26) and (27) was modified by multiplication by this additional taper factor $T(\xi)$, and though it may be claimed that the expression for $T(\xi)$ is not entirely in accordance with the assumed polar diagram factor (25), the discrepancy is not regarded as significant.

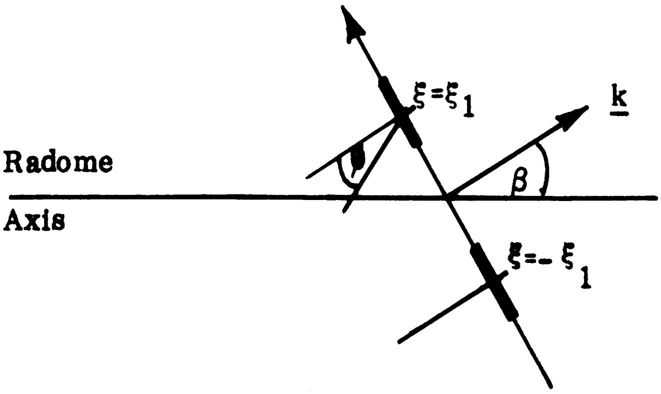

Fig. 6: Monopulse Geometry.

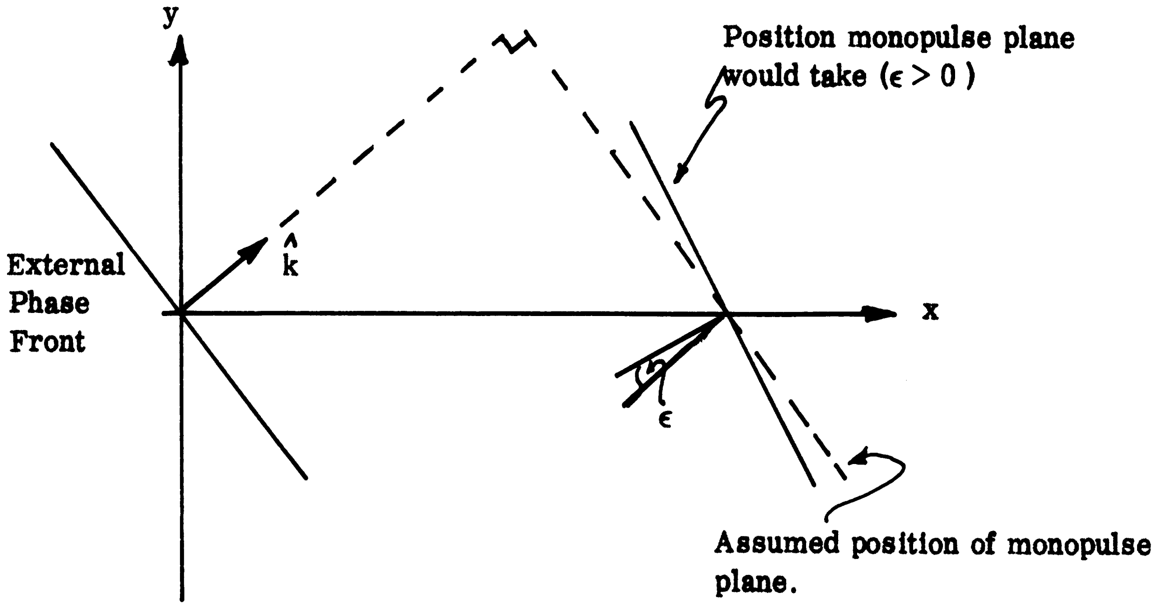

Fig. 7: Pointing Error Geometry.

V EFFECT OF A SURROUNDING (WEAK) PLASMA

Under some conditions of operation the radome may be surrounded by a weak plasma that can be treated as lossless, and this modification to the external environment can affect the pointing error of the system. Any change of this type will be a function of the plasma characteristics and, hence, of the height and velocity of the vehicle, and may constitute a more severe problem than the pointing error for the bare radome. It is feasible (and, indeed, common practice) to attempt to compensate for the latter error by either electronic or physical means (for example, by shaving or blocking-off portions of the surface in a manner determined by experiment), but this would be ineffective for an error which was a variable function of position along a trajectory of the vehicle. Moreover, were the plasma-induced effect to serve to decrease the pointing error when the radome were bare, complete compensation for the latter error could be undesirable. It is therefore appropriate to examine the change in pointing error produced by a plasma sheath or layer.

We first seek an expression for the equivalent refractive index of a plasma . In terms of the polarization vector $\underline{P}$, the displacement vector $\underline{D}$ is

$$\underline{D} = \epsilon_0 \underline{E} + \underline{P} \quad .$$

The movement of an electromagnetic wave through a plasma leads to a displacement of the electrons, and to the creation of effective dipoles. If there are N electrons per unit volume and if all move through the same distance $\underline{r}$ (parallel to $\underline{E}$) , the equivalent dipole moment per unit volume is

$$\underline{P} = N e \underline{r}$$

where e is the charge on an electron.

The equation of motion of an individual electron in the absence of an imposed magnetic field, but taking account of collisions, is

$$m \frac{\partial^2 \underline{r}}{\partial t^2} + m\nu \frac{\partial \underline{r}}{\partial t} = e\,\underline{E}\,,$$

where ν is the average frequency of collisions between electrons and heavy particles. Hence, with a time dependence $e^{-i\omega t}$,

$$\underline{r} = - \frac{e\,\underline{E}}{m\omega\,(\omega + i\nu)}$$

giving

$$\underline{P} = - \frac{N e^2}{m\omega(\omega + i\nu)}\,\underline{E}\,,$$

so that

$$\underline{D} = \left(\epsilon_o - \frac{Ne^2}{m\omega(\omega + i\nu)}\right)\underline{E}\,.$$

The equivalent permittivity is therefore

$$\epsilon = \epsilon_o\left(1 - \frac{Ne^2}{m\epsilon_o\omega(\omega + i\nu)}\right)$$

and taking $\mu = \mu_o$, the equivalent refractive index is

$$n = \left(1 - \frac{Ne^2}{m\epsilon_o\omega(\omega + i\nu)}\right)^{1/2} \quad . \tag{34}$$

If, as we shall assume, any losses in the plasma can be neglected, $\nu = 0$. It is then convenient to define a radian plasma frequency ω_p such that

$$\omega_p^2 = \frac{Ne^2}{m\epsilon_o}\,, \tag{35}$$

in terms of which

$$n = \left(1 - \frac{\omega_p^2}{\omega^2}\right)^{1/2} \quad . \tag{36}$$

It will be observed that for $\omega > \omega_p$ the refractive index is real (as expected) and $0 < n \leq 1$. Some idea of its magnitude can be obtained by inserting the magnitudes of e, m and ϵ_o into (35). With

$$e = -1.6021 \times 10^{-19} \text{ coulombs} ,$$

$$m = 9.108 \times 10^{-21} \text{ kgm.},$$

$$\epsilon_o = \frac{10^{-9}}{36\pi} \text{ farads/m .},$$

we have

$$\omega_p = 5.64 \times 10^4 \sqrt{N} \text{ radians} ,$$

where N is here the number of electrons per cc. When expressed in terms of cycles/sec ($\omega_p = 2\pi f_p$) ,

$$n = \left(1 - \frac{f_p^2}{f^2}\right)^{1/2} \tag{37}$$

with

$$f_p = 8.98 \times 10^3 \sqrt{N} \text{ Hz} , \tag{38}$$

and hence, at C-band (f = 5 GHz),

$$n = (1 - 3.22 \times 10^{-12} N)^{1/2} \quad . \tag{39}$$

Some typical values of 1-n are as follows:

$N = 10^{8}$	$1-n = 1.61 \times 10^{-4}$
5×10^{8}	8.05×10^{-4}
10^{9}	1.61×10^{-3}
5×10^{9}	8.08×10^{-3}
10^{10}	1.62×10^{-2}
5×10^{10}	8.40×10^{-2}
10^{11}	1.77×10^{-1} .

We note that for $N \leq 5.9 \times 10^{10}$, $n \geq 0.9$ and that for $N < 2 \times 10^{10}$, n can be approximated by the expression

$$n \simeq 1 - 1.61 \times 10^{-12} N \tag{40}$$

with at least three digit accuracy. The largest value of N in the electron density profiles which have been furnished us is 10^{10}, and accordingly, from the above Table, $n \geq 0.984$.

The presence of the plasma outside the radome will modify the rays which would have impinged on the radome in the absence of the plasma, and in order to extend the bare-radome treatment to this case, we must now examine the perturbation of the rays on passing through the plasma. Since the electron density and, hence, refractive index is a function of distance normal to the radome surface throughout the sheath, the only practical method of ray tracing is to assume that the plasma is locally stratified parallel to the surface and to ignore the reflection from the stratification layers. This is the usual technique for ray tracing through a region of variable refractive index (e.g. the atmosphere), and because of the relatively small maximum variation in n, it might be thought that the procedure is unquestionably valid . In the present problem, however, the variation in n takes place within a layer whose thickness is no more than $\lambda/6$ and can be as small as $\lambda/60$. The criterion for neglecting subsidiary reflections, i.e. for assuming each ray to proceed undiminished, is

$$\frac{\cos\alpha}{k}\ \frac{\partial n}{\partial y} << 1\,, \tag{41}$$

where y is measured normal to the stratification and α is the angle which the incident ray makes with respect to the normal. For the data furnished to us, the maximum values of $\partial n/\partial y$ occurs near to the nose of the radome where the electron density is largest and the layer is thinnest. We have

$$\max \frac{\partial n}{\partial y} \simeq (3 \times 10^{10} \times 1.61 \times 10^{-12}) \Big/ (\text{min. layer thickness})$$

$$= \frac{2.9}{\lambda}\ \text{inch}^{-1}$$

and hence

$$\max.\ \frac{1}{k}\ \frac{\partial n}{\partial y} \simeq 0.46\ .$$

In view of the fact that over most of the sheath, $\partial n/\partial y$ is a great deal less than its maximum value, and that under most circumstances a wave will strike the region of the maximum at a rather oblique angle, it is legitimate to conclude that the criterion (41) is fulfilled, albeit to a somewhat less degree than might have been expected from a consideration of the change in refractive index alone. More to the point, perhaps, is the fact that to proceed on any other basis would produce a problem of forbiddable complexity.

As a result of traversing a slowly varying medium of this type, a ray will reach the surface of the radome with its amplitude undiminished, but with its phase, impact point and (possibly) direction changed from what they would have been had the plasma not been present. To compute these modifications, we postulate a planar stratification of the region traversed by any given ray, as shown in Fig. 8. Let y be the coordinate normal to the stratification (and to the local radome surface), and n = n(y) be the refractive index throughout the plasma layer of thickness t. For the moment we assume that the region $y < 0$, as well as $y > t$, is free space with refractive index unity, and choose origin of coordinates at that point on the surface $y = 0$ which a ray incident on the outer surface of the layer at an angle α to the normal would have reached in the absence of the layer. The coordinates of the point (x_1, y_1) at which the ray strikes the lower surface of the layer are therefore

$$x_1 = -t \tan\alpha, \quad y_1 = t \quad . \tag{42}$$

From Snell's law

$$n(y) \sin\beta = \sin\alpha \ , \tag{43}$$

where β is the local inclination to the vertical of the ray path within the layer. If ds is an element of distance along the ray path, the horizontal distance of travel within the layer is

$$\int_{y=t}^{y=0} ds \sin\beta = -\int_t^0 dy \tan\beta = \int_0^t \frac{\sin\alpha}{\sqrt{n^2-\sin^2\alpha}} \, dy \ ,$$

and the x-coordinate of the point at which the ray strikes the plane $y = 0$ is now

$$x_0 = \sin\alpha \int_0^t \left\{ \frac{1}{\sqrt{n^2-\sin^2\alpha}} - \sec\alpha \right\} dy \ . \tag{44}$$

The (optical) distance traversed by the ray within the layer is likewise

$$\int_{y=t}^{y=0} n ds = -\int_t^0 \frac{n dy}{\cos\beta} = \int_0^t \left\{ \sqrt{n^2-\sin^2\alpha} + \frac{\sin^2\alpha}{\sqrt{n^2-\sin^2\alpha}} \right\} dy \ ,$$

$$= (x_0 - x_1)\sin\alpha + \int_0^t \sqrt{n^2-\sin^2\alpha} \, dy \ ,$$

and thus the excess of optical distance over that of the ray in the absence of the plasma is

$$\delta \ell = x_0 \sin\alpha + \int_0^t \left\{ \sqrt{n^2 - \sin^2\alpha} - \cos\alpha \right\} dy \quad . \tag{45}$$

If the quantities x_0 and $\delta \ell$ were computed as functions of α, t and n(y), the most obvious procedure for extending the bare radome procedure to the case in which the plasma was present would be to follow any individual ray from the wavefront to the outer surface of the radome ignoring the plasma, and then displace the ray laterally by the (small) amount x_0 and increase its phase by $k\delta\ell$. Since the plasma is actually in contact with the surface of the radome, there is also a slight change in direction of the impinging ray from α to α' , where $\alpha' = \sin^{-1}\left(\sin\alpha / n(0)\right)$, and an associated change in the reflection and transmission coefficients. For convenience, and because the electron density in general decreases in the immediate vicinity of the radome surface, these effects will be ignored: this is tantamount to conceiving of a small air gap between the inner plasma surface and the radome, and allows us to make full use of the original computation procedures for a bare radome, providing the quantities x_0 and $\delta \ell$ can be determined.

In their 'exact' forms given in Eqs. (44) and (45), the evaluation of the expressions for x_0 and $\delta\ell$ requires a knowledge of the variation of the refractive index n as a function of y, leading to numerical integrations, but if α is not too close to $\pi/2$, the two formulae can be simplified to a considerable extent. Since

$$n^2 - \sin^2\alpha = \cos^2\alpha - (1-n^2)$$

we have

$$(n^2 - \sin^2\alpha)^{-1/2} \simeq \sec\alpha \left\{ 1 + \frac{1}{2}(1-n^2)\sec^2\alpha \right\}$$

providing

$$\cos^2\alpha \gg 1 - n^2 \; ,$$

and hence

$$x_0 \simeq \frac{1}{2}\tan\alpha\,\sec^2\alpha\int_0^t (1-n^2)dy = 1.61\times 10^{-12}\tan\alpha\,\sec^2\alpha\int_0^t N\,dy, \tag{46}$$

which involves only the integrated electron density through the layer. The fact that x_0 is positive is consistent with a deviation of the wave away from the normal (n being less than unity). Similarly,

$$\delta\ell \simeq x_0\sin\alpha - \frac{1}{2}\sec\alpha\int_0^t (1-n^2)dy = -1.61\times 10^{-12}\sec\alpha(1-\tan^2\alpha)\int_0^t N\,dy \tag{47}$$

and thus

$$\delta\ell \simeq -\cos 2\alpha\,\mathrm{cosec}\,\alpha\, x_0 \; . \tag{48}$$

Since $x_0 > 0$, $\delta\ell$ is negative or positive according as α is smaller or greater than $\pi/4$, respectively.

To make use of the formulae (46) and (47), we now turn to the data for plasma layer thickness and electron density that have been furnished us. The boundary layer thickness t measured normal to the outer surface of the radome at an axial distance x_1 from the nose is represented by

$$t = \begin{cases} 0.01227x_1^{0.5} + 0.0012 \;, & 0 \le x_1 \le 10 \\ 0.012x_1 - 0.08 \;, & 10 \le x_1 \le 15 \\ 0.0224\,x_1^{0.8} - 0.0958 \;, & 15 \le x_1 \le 48 \end{cases} \tag{49}$$

where all dimensions are in inches. In terms of the coordinate system of Fig. 4,

$$x_1 = x - \ell \; .$$

Note that

$$t(10)=0.04, \quad t(15) = 0.10, \quad t(48)= 0.40 \ .$$

The electron density varies as a function of distance y normal to the radome surface throughout $0 \leq y \leq t$, but does so in a manner that depends on x_1. Data curves* for $N=N(y)$ (electrons/cc) as functions of $\bar{y} = y/t$ are shown in Fig. 9.

From Eq. (46) it is observed that the approximate expression for the lateral displacement x_0 of the intercept point with the radome surface is proportional to

$$\int_0^t N(y)\, dy = t\, I \qquad (50)$$

where

$$I = \int_0^1 N(\bar{y})\, d\bar{y} \ . \qquad (51)$$

Since $N(\bar{y})$ depends on the particular range of x_1 (see Fig. 9), I likewise differs in the four ranges, but its value for each can be obtained by numerical integration of the corresponding curve in Fig. 9. But fitting log N to a polynomial form and then integrating numerically, it is found that

$$I = \begin{cases} 2.039 \times 10^9 & \text{for } 0 \leq x_1 < 5 \\ 2.223 \times 10^8 & \text{for } 5 < x_1 < 10 \\ 1.147 \times 10^8 & \text{for } 10 < x_1 < 20 \\ 6.962 \times 10^8 & \text{for } 20 < x_1 < 48 \ . \end{cases}$$

Knowing I and t (see Eq. 49) for the various ranges of x_1, the integrated electron density is obtained from Eq. (50) and the lateral displacement x_0 for any given α then follows from Eq. (46). The change in optical distance is trivially related to x_0 through Eq. (48).

---

*Private communication with Dr. I. Pollin, 13 November 1968.

To assess the accuracy of the approximate formulae (46) and (48), we considered the actual electron density profile in Fig. 9 for the range $0 \leq x_1 < 5$, and evaluated numerically the precise integral expressions for x_0 and $\delta \ell$ in Eqs. (44) and (45) for a series of incidence angles α. The results are shown in the following Table along with the approximate values obtained from Eqs. (46) and (48).

TABLE

$\alpha(^o)$	Exact x_0/t	Approx. x_0/t	Exact $\delta \ell/t$	Approx. $\delta \ell/t$
10	6.082×10^{-3}	5.967×10^{-3}	-3.248×10^{-2}	-3.229×10^{-2}
20	1.381×10^{-2}	1.353×10^{-2}	-3.045×10^{-2}	-3.030×10^{-2}
30	2.590×10^{-2}	2.527×10^{-2}	-2.526×10^{-2}	-2.527×10^{-2}
40	4.845×10^{-2}	4.693×10^{-2}	-1.216×10^{-2}	-1.268×10^{-2}
50	9.911×10^{-2}	9.467×10^{-2}	2.408×10^{-2}	2.146×10^{-2}
60	2.458×10^{-1}	2.274×10^{-1}	1.456×10^{-1}	1.313×10^{-1}
70	9.257×10^{-1}	7.709×10^{-1}	7.682×10^{-1}	6.284×10^{-1}

Certainly for $\alpha \leq 60^o$ the agreement is rather good, and bearing in mind that we have here considered the case in which N achieves its maximum possible value 10^{10} (electrons/cc) and for which the discrepancies between the exact and approximate expressions are greatest, the results provide reasonable confidence in using (46) and (48). Only the integrated electron density is then relevant.

For $\alpha = 70^o$, the approximate expressions underestimate both x_0 and $\delta \ell$, and the discrepancies become more apparent as α increases. This is due to the considerable bending which a ray now undergoes . From Eq. (43) it is seen that the local inclination to the vertical will reach 90^o at a depth within the sheath such that $n(y) = \sin \alpha$; and having become parallel to the radome surface, the ray will now emerge from the sheath without ever intercepting the radome. In the case considered above where the maximum value of N is 10^{10} (corresponding to n=0.9838), failure to intercept will occur for all $\alpha \geq 79.7^{o}$. Thus, for example, for a sheathed conical radome of half-angle 9.5^{o} illuminated at an angle within 0.8^{o} from axial incidence, no rays can penetrate the forward part where $0 \leq x_1 < 5$, but rays which strike further back where the peak electron density is less will be able to get through.

Although the accuracy of the approximate formulae (46) and (48) is not entirely adequate for $\alpha > 65^{o}$ (say), the time that would be involved in performing the numerical integrations demanded by (44) and (45) for each and every ray makes the use of the simplified expressions most desirable, if not mandatory. Having said this, it should be noted that for any given (large) angle α, the 'error' implied by (46) and (48) decreases with the peak electron density and could in any case be removed by employing an integrated electron density (or layer thickness) somewhat greater than is implied by the curves in Fig. 9. Since it is presumed that such an 'adjustment' is small compared with the inherent uncertainty associated with the data in Fig. 9, Eqs. (46) and (48) will be employed without any modification.

It is now a rather straightforward matter to take into account the presence of the plasma. Any given ray is first traced to an intercept with the radome as though the plasma were not there. Knowing the value of x (and hence x_1) appropriate to this intercept, x_0 and $\delta \ell$ are computed. The intercept point is then displaced by a distance x_0 along the surface of the radome and the optical distance increased by $\delta \ell$, and the ray is traced through the radome in the same manner as before. It should be emphasized that x_0 is a displacement along the surface, rather than in the x direction as such. This is trivial to execute for a conical radome; for the ogival one, x_0 is treated as an arc length, and the intercept is formed by constructing a circle of radius x_0 about the point at which the ray strikes the radome in the absence of the plasma. Of the two possible intercepts of this circle with the radome, that for which x is larger is selected.

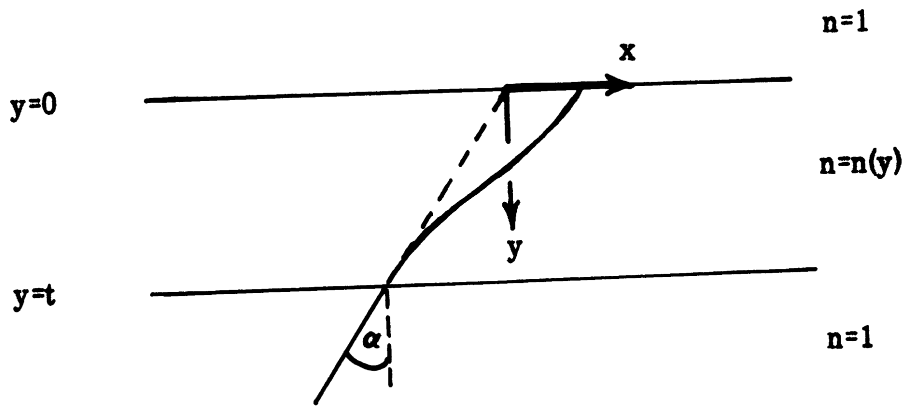

Fig. 8: Local Geometry of the Plasma Layer.

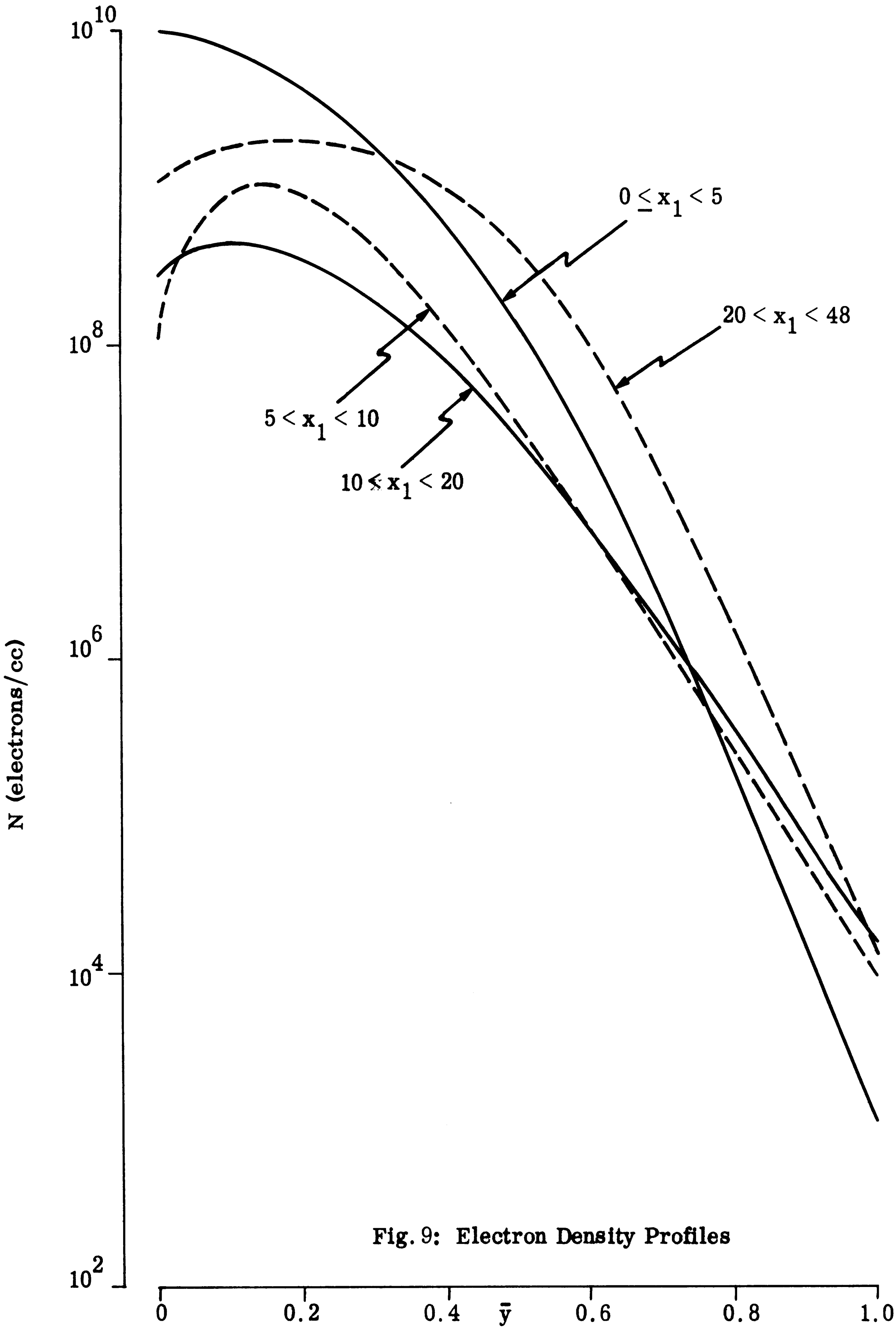

Fig. 9: Electron Density Profiles

VI NUMERICAL PROCEDURES AND RESULTS

Before going on to present the specific numerical results that have so far been obtained with our numerical program, there are a few points concerning the manner in which the incident wave front is sampled that should be enlarged upon.

In Section IV we discussed the need to 'smooth' the change in the induced signal in a slot when a primary ray just hits a slot as opposed to when it just misses, and we noted that a reasonably effective (and realistic) procedure is to incorporate an amplitude taper in each slot response function. This has the effect of enabling us to sample the incident wave front at a lower rate than would otherwise be the case, but still leaves us with the task of determining what is an 'optimum' sampling rate; by 'optimum' we here mean one that will minimize the computation time (i.e use a minimum number of sampling points) and still yield values for the pointing error of sufficient accuracy.

In order to obtain data from which to estimate the optimum rate, we chose to consider a bare ogival radome for an H-polarized (or TM) wave incident at 30^{o} from nose-on. To judge from a variety of data sets then available, this case appeared satisfactory for test purposes. Pointing errors were now computed for various stepping distances, Δ (in inches) along the wave front as a function of the position of the starting point for the first (lowest*) ray. Thus, for a given Δ and a given starting point, ϵ was computed. The starting point was then displaced a distance $\Delta/10$ upwards, and the process repeated; and so on until, after 10 such displacements, the starting point in the 10th case coincided with that of the second ray in the first case. It was found that the pointing error was a smooth oscillatory function of the displacement, with one complete cycle corresponding to 10 displacements. For $\Delta = 0.05$ (inches), for example, ϵ varied from

*In the program, sampling starts at the lowest point and works up the wavefront.

9.82 to 9.99 milliradians, whereas for $\Delta = 0.2$, the variation was from 9.85 to 10.14 milliradians. It was felt that an uncertainty of ± 0.15 milliradians was an acceptable accuracy, and since such factors as the weighting applied to the slots had no real effect on the variation of ϵ, we therefore settled on a rate of sampling of the incident wave front corresponding to a stepping distance of 0.2 inches along it. This same value of Δ has been employed in the 3-dimensional program, and whereas in the present case the increase in Δ from 0.05 to 0.2 inches reduces the number of rays (and hence the running time of the program) by a factor 4 — an improvement which is certainly not negligible, the improvement in the 3-dimensional program is by a factor 16 and is considerable.

The next topic to be discussed is the choice of the initial or starting point at which the incident wave front is sampled. The ray tracing program is designed to start with the lowest ray which can produce an intercept with the monopulse plate, and then to step up along the wave front through a chosen distance Δ a specified number of times. The starting point is taken to be the projection of the lowest point of the monopulse plate on to the incident wave front (see Fig. 10): consideration of the refractive effect of a convex radome shows that no lower ray could conceivably provide an intercept. We can similarly specify an uppermost sampling point by projecting the top of the monopulse plate and by finding that point from which a ray is tangent to the upper surface of the radome (in the case of a conical radome, the latter point is replaced by the projection of the radome tip). The upper of these two points consitutes the final sampling point, and the number, N, of increments is then obtained by dividing the wavefront distance (in inches) by Δ.

Another matter of some importance is the cut-off or tolerance criterion that is adopted. As each ray undergoes successive reflections and transmissions, its amplitude decreases and ultimately falls to a level at which its contribution can be neglected without significant error. Although one would prefer to set this level as low as possible, to do so could increase the computation time without any marked improvement in accuracy. A rather wide variety of test cases were run in which the tolerance was set at anything between 0.001 and 0.05, i.e. in which rays were abandoned when their amplitude had decreased to less than 0.1 percent and 5 percent, respectively, of their initial value (unity). It was found that decreasing the tolerance from 0.01 to 0.001 affected the pointing error by no more than 0.2 or 0.3 milliradians, and though the tolerance criterion was preserved as one of the input parameters, it was set at 0.01 in all subsequent runs. It may be noted here that this same level has been adopted in the 3-dimensional program.

In the description of the monopulse system given in Section IV, we allowed for the possibility of differential weighting factors applied to the various slots. The weighting factors that are appropriate depend, of course, on the manner in which the slots are connected, but to get a general feeling for the extent to which they can affect the pointing error, a series of tests was run using four symmetrical slots with either equal weighting or with the outer slots weighted by a factor 1/2 relative to the inner ones. It was found that such a decrease in the sensitivity of the outer slots increased the pointing error, the change being of order 10 percent.

The final form taken by the 2-dimensional computer program is rather general, and permits the computation of the pointing error for either a TE or TM plane wave at any angle of incidence on a radome whose surfaces are specified by either linear or quadratic equations, with or without a surrounding (weak) plasma, and for a variety of monopulse plate configurations. A complete list of the input variables and their format is given in the Appendix (Even though this list may seem quite lengthy, only 4 cards are needed for each set of data, and for a typical modification of input parameters such as a change in the incidence angle of the wave, only one of these cards has to be altered.

Numerical Results

In order to test out the programs and, at the same time, to obtain explicit values for the pointing errors in cases of some practical interest, complete runs were carried out for two particular radome and slot configurations with and without a plasma present.

The incident field was (as always) assumed to be a plane wave having either its electric or magnetic vector in the z-direction (TE or TM polarized waves, respectively) and incident at an angle β to the radome axis varying from 0^o (axial incidence) to 55^o. The (free space) wavelength was taken as 2.4 inches, corresponding to a frequency 4.918 GHz. The radome material was treated as a homogeneous isotropic dielectric with permeability $\mu = \mu_o$. Thus,

$$n \equiv \sqrt{\frac{\epsilon}{\epsilon_o}} = 2.5 ,$$

which is typical of the refractive index of fiberglass in the microwave range.

The monopulse plate was assumed to consist of 4 symmetrical slots centered at $\pm$ 2.4 inches and $\pm$ 4.8 inches from its mid-line, and having widths 2d=1.2 inches. The slots were weighted equally and had a cosine amplitude taper associated with each. For simplicity, the individual slot voltages were not printed out, and the output therefore consisted of only a single pointing error ϵ (in radians) arrived at in the manner described in Section IV.

The plasma (when present) was taken to have the characteristics provided by Dr. I. Pollin (personal communication) and listed in Section V.

The two particular radomes that were considered are the two-dimensional analogues of those described by Dr. Pollin (loc. cit.). The first is a two-dimensional conical (or wedge) radome (see Fig. 11a) whose outer and inner surfaces are given in terms of the coordinates of Fig. 4 by the equations

$$y = \pm \frac{1}{6} (x-1), \qquad y = \pm \frac{1}{6} (x - 4.191) ,$$

respectively, where all dimensions are in inches and the upper (lower) sign refers to the upper (lower) surface. The half-angle of the cone is approximately 9.5^o, and thus, in Eq. (16),

$$a = \frac{1}{6}, \quad \ell = 1 \text{ (outer)}$$
$$= 4.191 \text{ (inner)} .$$

The mid point of the monopulse plate is at x = 43.

The second radome considered is a two-dimensional ogive each of whose surfaces is formed by the rotation of a cylindrical arc about a chord (Fig. 11b). Each surface is defined by an equation of the form (15) with

$$A = 140, \qquad B = 48, \qquad C = 49$$

for the outer surface, and

$$A = 140, \qquad B = 45.832, \qquad C = 49$$

for the inner surface. The half angle of the (outer surface of the) radome at its tip is approximately 18.4^{o}, and the monopulse plate is situated at x = 39. It should be noted that for neither radome have we postulated any tip rounding.

The program was run first for the bare conical radome for each of the two polarizations, and with the angle of incidence β varying from 0^{o} to 55^{o} in 5^{o} steps. When it was found that the pointing error, ϵ, varied rather rapidly in certain ranges of β, computations were carried out for additional values of β in order to pinpoint the oscillations more precisely, and we ultimately ran the program at increments of 1^{o} in β for portions of the entire range. Analogous computations were then performed with the plasma present. A complete listing of the pointing errors (in milliradians) for the conical radome, with and without the plasma sheath, are given in Table 1, and the results for the bare conical radome are plotted as functions of β in Fig. 12. Attention was then turned to the ogival radome, and the pointing errors computed without the plasma present. Because rapid variations in ϵ now existed throughout the entire range of β (the source of these variations will be discussed in a moment), it was felt desirable to compute ϵ for no more than 1^{o} increments in β over most of the range, and even smaller increments were employed over a limited region. The results for the bare radome with TM polarization are plotted in Fig. 13, and a partial listing of these data and of the analogous results in the presence of the plasma, is given in Table 2. Due to lack of time and money, no comparable runs were carried out for the ogival radome with TE polarization.

Table 1: Conical Radome Pointing Errors (Milliradians)

β(deg.)	Bare TE	Bare TM	With Plasma TE	With Plasma TM	Plasma-Bare TE	Plasma-Bare TM
0	0.00	0.00	0.00	0.00	0.00	0.00
1	2.13	2.42	-0.13	0.02	-2.26	-2.40
2	4.47	4.80	-1.63	-0.80	-6.10	-5.60
3	6.20	7.08	-10.93	-8.21	-17.13	-15.29
4	4.36	5.16	-18.97	-16.96	-23.33	-22.12
5	5.28	6.01	-15.05	-0.80	-20.33	-6.81
6	6.25	7.25	0.35	11.52	-5.90	4.27
7	-2.70	-4.96	10.85	18.31	13.55	23.27
8	0.39	0.00	-0.51	0.95	-0.90	0.95
10	0.36	0.00	-0.19	-0.56	-0.55	-0.56
11	0.42					
12	3.77					
13	10.72	-0.07				
14	10.57		10.34		-0.23	
15	-11.62	-0.86	-11.54	-0.75	0.08	0.11
16	-14.67					
17	-10.22					
18	-7.18					
19	-4.46					
20	-2.53	0.23	-2.13	0.23	0.40	0.00
25	-0.24	0.11	-0.25	0.11	-0.01	0.00
30	-1.42	0.00	-1.42	0.00	0.00	0.00
35	-0.48	-0.15	-0.48	-0.14	0.00	0.01
40	-3.40	0.43	-3.42	0.41	-0.02	-0.02
45	0.12	0.07	0.11	0.07	-0.01	0.00
50	0.96	0.17	0.95	0.17	-0.01	0.00
55	-0.13	0.05	-0.05	0.11	0.08	0.06

Table 2: Ogival Radome Pointing Errors (Milliradians)

β(deg.)	TM Bare	TM Plasma	Plasma-Bare
0	0.00	0.00	0.00
5	1.20	0.44	-0.76
10	-10.21	-9.15	1.06
15	4.98	5.64	0.66
20	5.90	5.65	-0.25
25	5.17	5.27	0.10
30	-9.99	-9.97	0.02
35	5.03	5.08	0.05
45	4.43	4.66	0.23

Discussion of Results

Inspection of the results that have been obtained shows that in all instances the pointing error is a rather rapidly varying function of the incidence angle β and except for the conical radome with $\beta \gtrsim 20^{o}$ the peak excursions are much larger than the 2 milliradian limit that was hoped for. This is true independently of the presence (or otherwise) of the plasma sheath. It is our belief that these features are real and that the results are not a reflection of the approximation inherent in using ray tracing.

In support of this belief, we examined in some detail the pointing errors that were obtained for the bare conical radome (see Fig. 12). Since the geometry is rather straightforward in this case, it was possible to trace manually the paths followed by the primary rays (which are the source of the dominant portion of the monopulse excitation) over various portions of the angular range. As expected from symmetry considerations, the pointing error is zero for nose-on incidence. As β increases from zero, the difference in path length between rays which have passed through the upper and lower radome walls also increases, and this in turn leads to an increasing phase difference between the excitations which the upper and lower slots receive. The pointing error therefore increases, and does so in a manner almost independent of polarization. With increasing β, however, even the upper slots begin to receive the bulk of their excitation from rays that have passed through the lower radome wall, and ϵ now decreases* from a peak value of $6 \sim 7$ milliradians to (effectively) zero for $\beta = 9 \sim 10^{o}$ when the rays are at glancing incidence on the upper wall. As β increases still further, we start receiving reflections off the upper (interior) radome surface,

*The 'overshoot' occurring in the 7 to 8^{o} range is attributable to internal reflections within the lower radome wall. Geometrical considerations show that the reflected waves will affect the slots differentially, leading to a rather localized pointing error which is polarization dependent (as observed).

and since the reflection coefficients for the TE polarization greatly exceed those for TM, significant differences between the two polarizations now occur. Indeed, for $\beta \geq 9^o$, the pointing error for the TM case remains less than 1 milliradian and, as such, is not much greater than the expected accuracy attainable from the computational procedure. In contrast, however, the strong wall reflections in the TE case produce a pointing error which rapidly increases for $\beta > 11^o$ and reaches a maximum of about 11 milliradians for $\beta = 13^o$. To begin with, only the upper slot(s) receive this perturbation signal, and because of the relatively small path difference between the direct and reflected 'waves', the pointing error is positive (see Fig. 7). But with increasing β the path difference becomes significant and the pointing error changes rapidly to a negative value. It is the phase (or path) difference which is primarily responsible for this, and the effect is analogous to a 'hunting' action on the part of the monopulse. The peak (negative) ϵ is nearly -15 milliradians, and occurs for $\beta = 16^o$. As β increases still further, the pointing error decreases, partly due to the increasingly uniform illumination of the monopulse plane by the reflected wave, but more importantly because of the decreasing effect of the perturbation arising from the progressive reduction in the reflection coefficients and the suppresive action of the polar diagram associated with the slot response. Although ϵ continues to oscillate even for $\beta > 20^o$, it now does so with a much reduced amplitude, and it is not possible to pinpoint any single source for each individual peak.

The above interpretation of the dominant features of the curves in Fig. 12 was arrived at by a detailed examination of the ray contributions to the monopulse excitation, and by a few exercises with a ruler, protractor and a slide rule. The same general picture continues to hold when the plasma is present, and whilst the plasma can be expected to change some of the details as a result of its lateral non-uniformity and its modification to the rays that enter the radome, we should expect to see the same principal features in the pointing error curves. Inspection of Table 1 shows that this is the case. Note, however, that some of the pointing error peaks are reversed in sign (a phasing effect primarily), and because all tend to be slightly displaced in angle, the change in pointing error produced by the radome can be quite large particularly in the critical region near to nose on where the non-zero values of ϵ are almost completely due to a phase (or path difference) effect. For $\beta \gtrsim 15^{o}$, the plasma produces no significant change in ϵ .

The understanding resulting from the above 'dissection' of the results for the conical radome enables us to appreciate why it is that the ogival radome displays the even more complicated behavior shown in Fig. 13. Since the half angle of the radome is now almost 19^{o}, we might expect that in this range the pointing error will oscillate in a similar manner to what it did for a conical radome when $0 \leq \beta < 9.5^{o}$. To at least some degree, this is indeed the case, but because of the curved geometry implying variations in reflection and transmission coefficients over different portions of the walls for even a fixed value of β, the detailed structure of the ϵ pattern is a great deal more complex than for the conical radome. Were it in isolation, the lower radome could no longer transmit a uniform plane wave, so that the monopulse plate receives a field of rather complicated structure even from this part of the radome alone. The situation is still worse for the upper wall. At any given angle of incidence, a single slot will see a dominant reflected wave coming from only that small portion of the wall which is appropriately aligned; and in consequence, both the phase and the direction of the dominant reflected signals will vary markedly from slot to slot. Under these circumstances it is not surprising that ϵ shows large and violent changes as a function of β , with each peak being attributable to the cumulative effect of many small contributions which themselves change rapidly from one value of β to the next. Un-physical as the results in Fig. 13 may appear, we have no reason to doubt them.

A comparison between the pointing errors with and without the plasma present is given in Table 2 for 9 isolated values of β . It is interesting to note that based on this small sample alone one would conclude that the plasma has less effect on ϵ for an ogival radome than it did for a conical one. There does not seem any obvious explanation for this.

Conclusions

In this Memorandum we have given a complete description of the numerical approach that we have adopted in determining the behavior of a monopulse system mounted within a 'two-dimensional' radome with or without a weak plasma sheath surrounding it. The theoretical foundations have been presented in some detail, as have the approximations which are necessary to permit the computations. Much of this is also appropriate to a treatment of a three dimensional radome, and we shall rely heavily on the present material when we come to describe the three-dimensional work.

The Appendix to this Memorandum contains a complete listing, flow chart and operating instructions for the two-dimensional numerical program, and we have given (and discussed) some of the results that have been obtained by applying it to two particular radome-monopulse configurations. These raise considerable doubt whether a 2 milliradian maximum pointing error for incidence angles out to 55° is an achievable objective regardless of the presence of a plasma sheath.

Although a two-dimensional geometry is, of course, a mathematical idealization, we believe that the program presented here is a valuable one in its own right and that the values of the pointing error obtained with it do represent a lower bound on those that would be found for the corresponding three-dimensional geometry. Certainly the program given here permits a much more rapid computation of ϵ than does the three-dimensional one, and whilst the present program was not written specifically for economy of operation (rather did we aim to permit the printing out of all intermediate data that might facilitate the understanding of the pointing errors found), the running (CPU) time in any one case (i.e. one angle of incidence, one polarization and one radome with or without plasma) varied from about 5 sec. to 20 sec. at most, depending on the particular circumstances. In contrast, the time for the three-dimensional program is two or more orders of magnitude greater.

Finally, it should be emphasized again that the entire approach has been based on ray theory and, in consequence, the results obtained are only approximate. Though it is our belief that the values found for the pointing error are accurate to within 1 milliradian, prudence would dictate that before complete reliance is placed on these data, some attempt be made to verify the conclusions experimentally. To do so for just the bare radome would be a valuable test, and it would not be hard to perform such an experiment using a simulated two-dimensional structure.

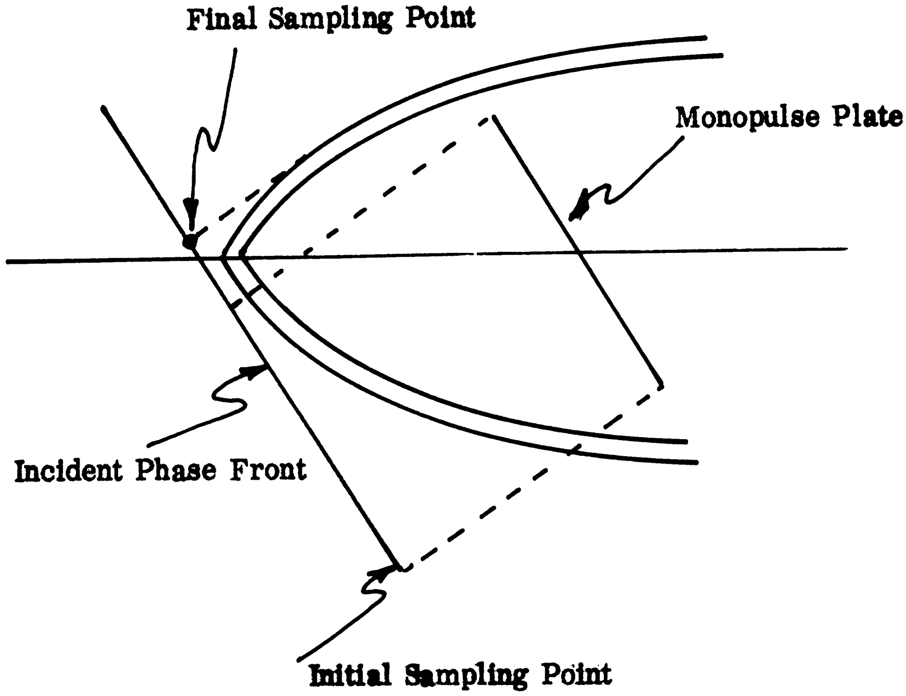

Fig. 10: Choice of Initial and Final Sampling Points.

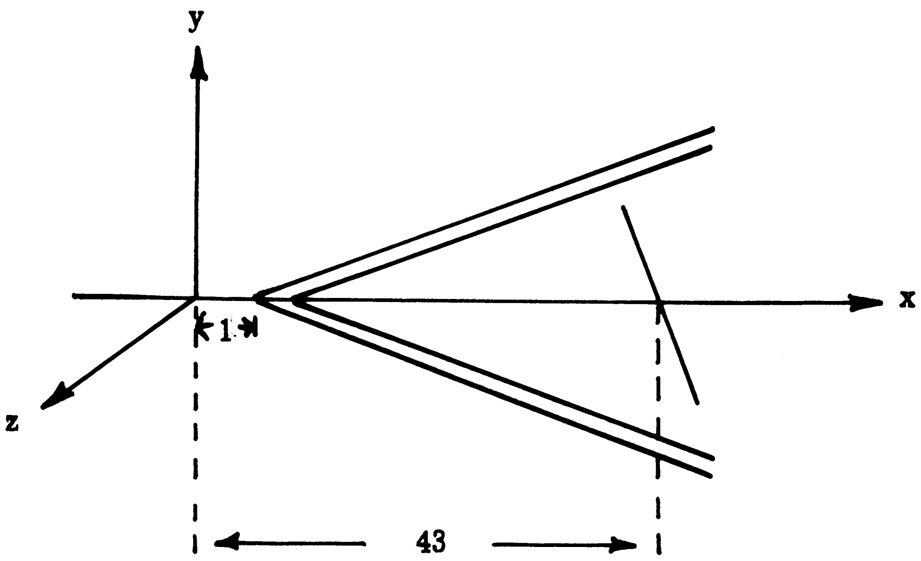

Fig. 11a: Conical Radome Geometry.

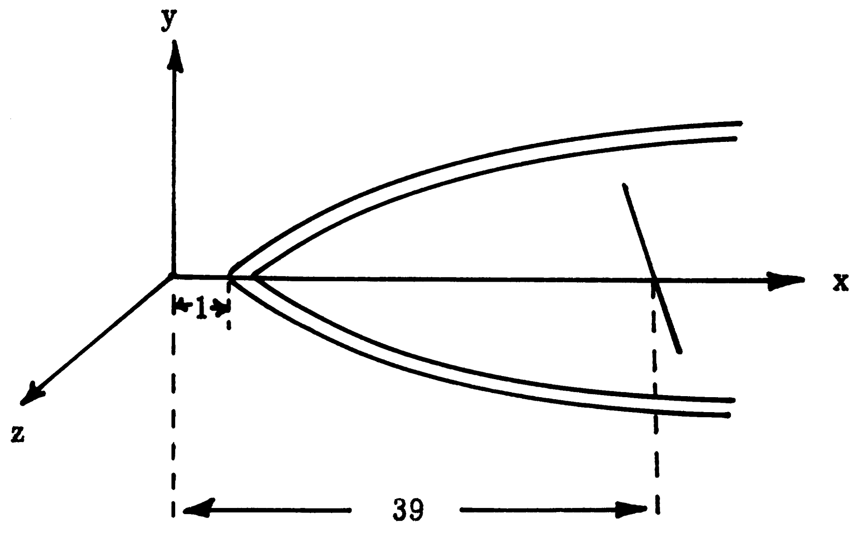

Fig. 11b: Ogival Radome Geometry

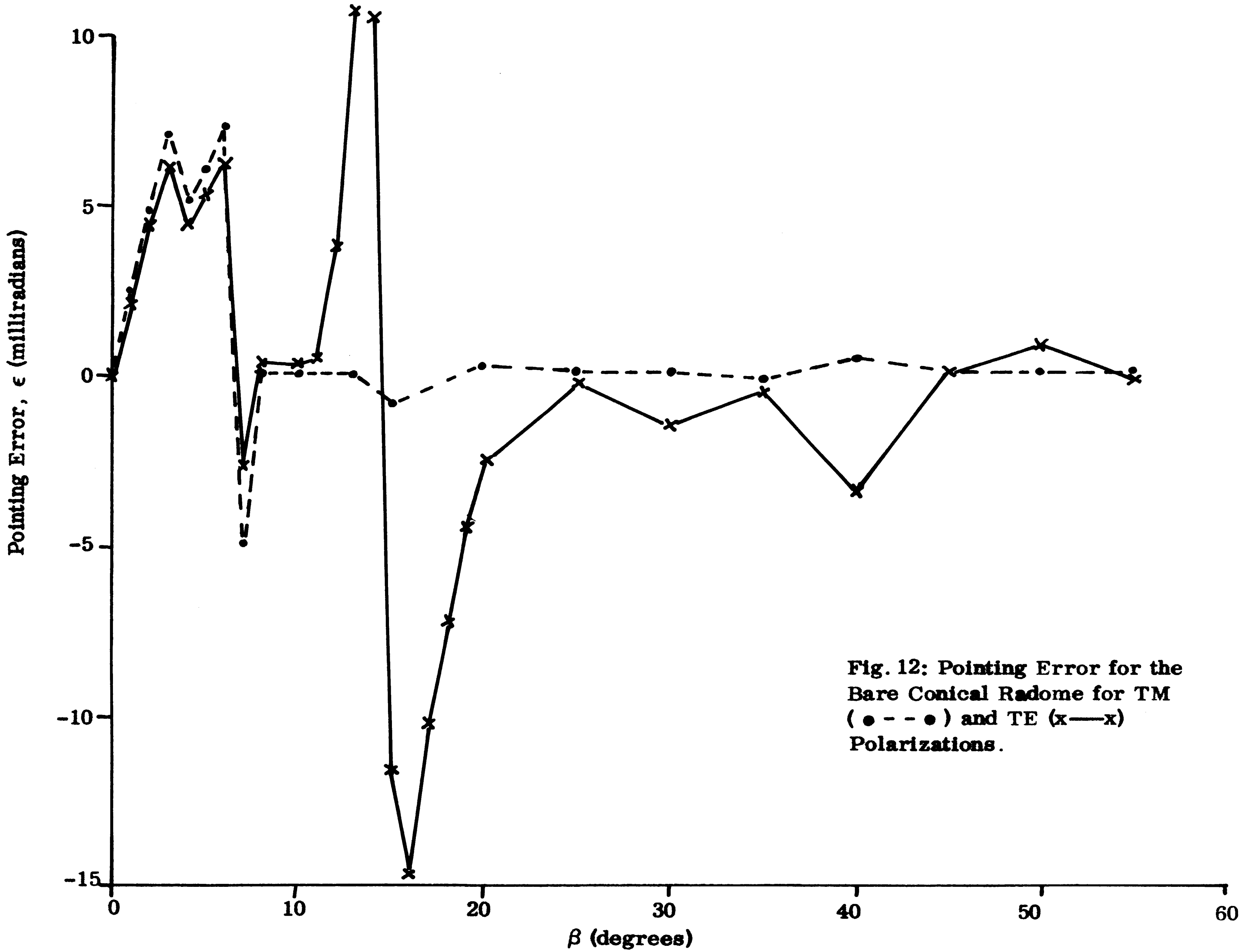

Fig. 12: Pointing Error for the Bare Conical Radome for TM (● - - - ●) and TE (x——x) Polarizations.

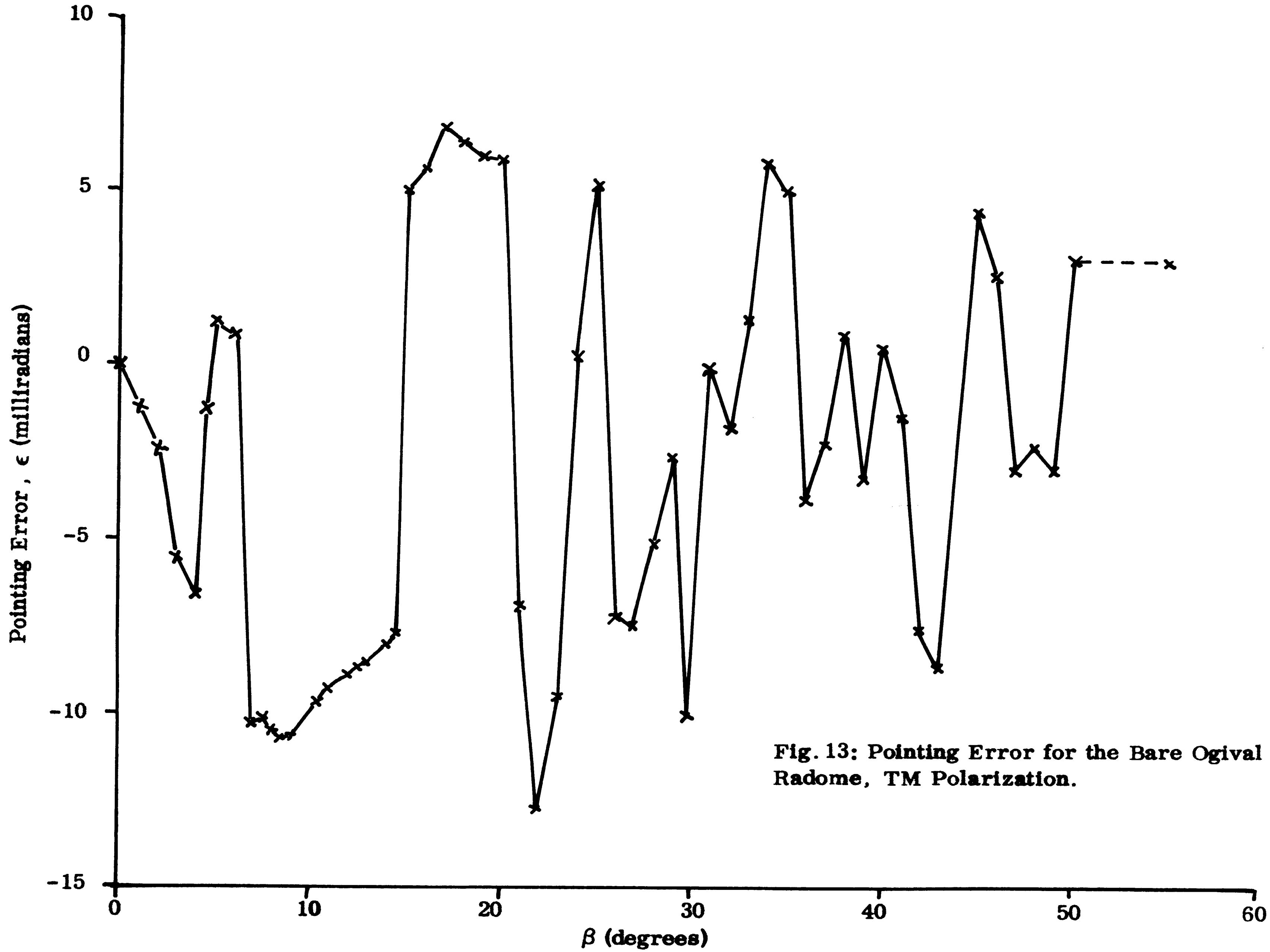

Fig. 13: Pointing Error for the Bare Ogival Radome, TM Polarization.

APPENDIX

FORTRAN COMPUTER PROGRAM

This description of the Fortran computer program consists of the following six parts:

(1) Usage hints and a complete description of the differences between the version for a conical surface and the version for a surface described by a certain quadratic function,

(2) Diagram showing terminology used in planning the program,

(3) List of input variables with their program code names and input card formats,

(4) List of Fortran source program,

(5) List of all variables used in program with code names and their meanings and usage, and

(6) Semi-detailed chart of logic flow in the program.

(1) Usage Hints

The program has been written to process an unlimited number of data sets, each data set consisting in form of data cards and resulting in a single pointing error, for a given aspect angle, frequency, polarization, geometry, and so forth. As a precautionary measure against incorrect data inputs a trap has been incorporated in the program to terminate the program when more than three errors are encountered in the input data.

The program, as it now exists, is by no means in its most efficient state. Storage requirements can be reduced by making changes to parts of the program which were included for flexibility and to aid in the program checkout. The dimensioning of variables ANGLE, AMPL, and DIST serves no purpose during current usage of the program. Also, some of the statements beginning near the statement numbered 370 may be eliminated by rearranging statements near the statement number 243 and then looping back sooner. This loop is performed each time a ray reflects in Region III.

Differences Between Quadratic and Conical Versions

Conversion of the computer program from one that handles the quadratic case where the surfaces are described by F1 and F2, segments of circles, to one which computes for the conical case where the surfaces are cones described by F1 and F2, straight lines, consists of the following steps (for the most part indicated in the card deck by comments).

1) The function

$$FX = ISIGN\ (\sqrt{A^2-(X-B)^2}-C\ )$$

becomes

$$FX = ISIGN^*(X-A)^*B\ .$$

The function

$$FDERX = \frac{ISIGN^*(B-X)}{\sqrt{A^2-(X-B)^2}}$$

becomes

$$FDERX = ISIGN^*B\ .$$

2) In the format number 171 the word "quadratic" becomes "conical".

3) In the plasma calculations the statement XB=XB+DELX(cos|arctan(DX)|) becomes XB-XB+DELX|cos(B)| and the statement XB=FZ(ZB) is eliminated.

4) The subroutine XPT is replaced with one which computes the point of intersection of straight lines.

Notice also that input variables A, B and C necessarily have different meanings.

(2) Diagram Showing Terminology Used in the Program.

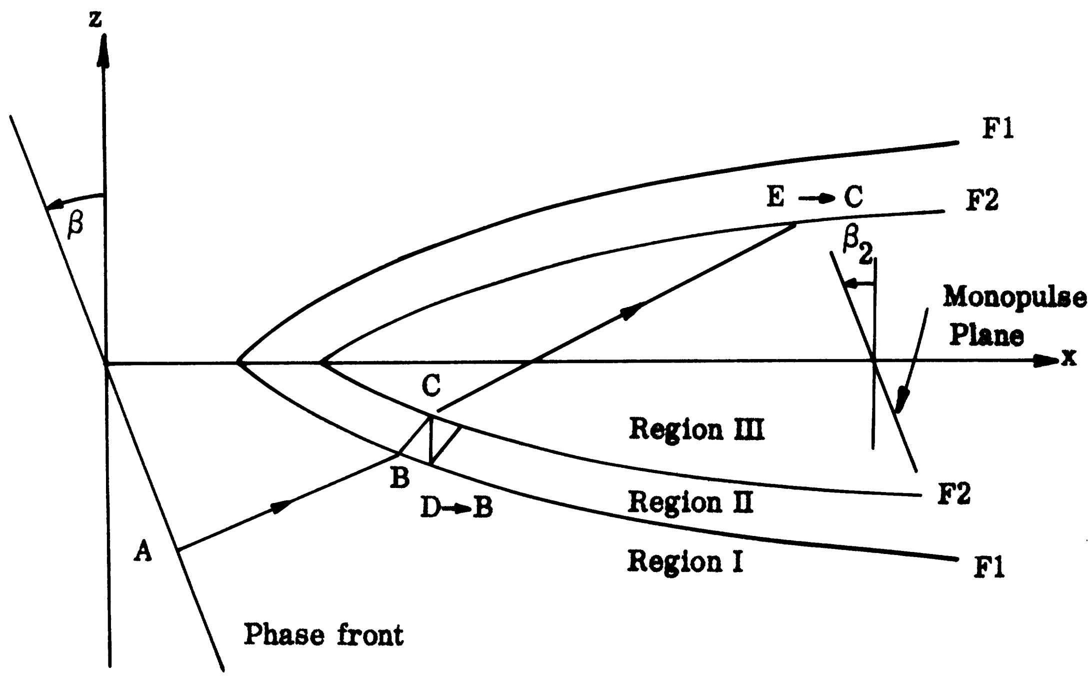

B is any point on F1.

C is point where a ray from point B hits F2.

D is a point of reflection on F1; it becomes point B after reflection calculations are made.

ISIGN = + 1 when intersection with top function is being sought,
= - 1 for bottom part.

IBELO is argument of call to subroutine XPT; indicates which point of intersection of surface with the circle is to be used (quadratic case);

≠ 2 means point used is upper if ISIGN is + and lower if ISIGN is - ;

= 2 : other point is used.

On return IBELO = 0 if intersection with a circle is found and if it is left of center of the circle determined by F.

(3) Input Variable List for FORTRAN Program

FORTRAN Name	Columns	Description
Card 1 - quadratic surface		
A	1-10	radius of circle described by radome (F1)
B	11-20	X-coordinate * of center of above circle
C	21-30	Z-coordinate of center of above circle
SMA	31-40	difference between radii of F1 and F2
Card 1 - conical surface		
A		X-coordinate of vertex of F1: outer surface
B		slope of top surface of cone
C		= 0 indicates case is conical
SMA		A- (X-coordinate of vertex (F2 = outer surface))
Card 2		
DELTA	1-10	increment used in stepping up radiating plane
TWON	11-20	refractive index of Region II
XZERO	21-30	X-coordinate of center (on X-axis) of receiving plane
BETA	31-40	angle (in degrees) of radiating plane to X-axis
BETA2	41-50	angle (degrees) of receiving plane to X-axis
ITEST	51-54	indicator which results in intermediate printing when set = 1
IPLAS	55-58	indicator = 1 when plasma present, 0 otherwise
NPRINT	59-62	indicator = 0 results in printing output whenever ray hits a slot; when set = 1 only pointing error is printed.

*All linear measurements are in inches.

Input Variable List for FORTRAN Program (continued)

FORTRAN Name	Columns	Description
Card 3		
Z1	1-10	Z-coordinate of first point on radiating plane
ZZERO	11-20	maximum distance from center of receiving plane that impacting rays will register (usually to top edge of top slot)
TOL	21-30	anytime the amplitude of a ray falls below this value, path tracing ceases for that ray
NUMINC	31-34	a maximum limit of the number of increments which will be stepped along radiating plane
TM	35-38	set = 1 for magnetic case; 0 otherwise
TE	39-42	set = 1 for electric case; 0 otherwise
Card 4		
WIDTH	1-10	half-width of slots on receiving plane
WAVEL	11-20	wavelength
APER(1 → 3)	21-30...	distance along receiving plane of centers of slots; bottom is symmetric
WEIGHT (1 → 3)	51-60...	weighting factors for up to 3 pairs of slots

(4) FORTRAN Source Program

```
FORTRAN IV G COMPILER          MAIN            11-28-69          12:17.25          PAGE 0001

0001              REAL N,MYO,MAG                                                            00110
0002              INTEGER TM,TE                                                             00120
0003              DIMENSION Z(30),APER(3),WEIGHT(6)                                         00130
0004              DIMENSION ANGLE(30),AMPL(30),DIST(30)                                     00140
0005              DIMENSION SUMX(6),SUMY(6)                                                 00150
            C  THE FOLLOWING STORAGE IS USED TO ACCUMULATE DATA OF REFLECTION POINTS        00160
            C     UNTIL IT CAN BE USED FOR COMPUTATION OF FINAL INTERCEPT POINT RESULTS 170
0006              DIMENSION SX(50),SZ(50),SM(50),SPHI(50),SD(50),ST(50),SR(50)              00180
            C  FUNCTION DEFINITIONS                                                         00300
0007              AP(ANG,AMP)=AMP*DK*COS(ANG)*                                              00310
                 1  (SIN(DK*SIN(ANG))/(DK*SIN(ANG)))                                        00320
0008              FX(I,A,B,C,X)=I*(SQRT(A*A-(X-B)*(X-B))-C)
0009              FDERX(ISIGN,A,B,X)=ISIGN*(B-X)/SQRT(A*A-(X-B)*(X-B))
0010              FZ(Z)=B+SQRT(A*A-(Z-ISIGN*C)*(Z-ISIGN*C))
            C  FUNCTION DESCRIPTIONS FOR CONICAL CASE                                       00350
            C  NOTE: ANOTHER VERSION OF SUBROUTINE XPT IS ALSO NEEDED                       00360
            C     FX(I,A,B,C,X)=I*(X-A)*B                                                   00370
            C     FDERX(ISIGN,A,B,X)=B*ISIGN                                                00380
            C  A= DISPLACEMENT OF VERTEX F1        B= SLOPE OF FUNCTION     C=0             00390
            C  (INPUT) SMA= VERTEX(F1)-VERTEX(F2); NOTE: A NEGATIVE VALUE                   00400
0011              FDIST(X1,X2,Y1,Y2)=SQRT((X2-X1)*(X2-X1)+(Y2-Y1)*(Y2-Y1))                  00410
0012              R22(GAM)=(1.-GAM)/(1.+GAM)                                                00420
0013              R33(GAM)=-(1.-GAM)/(1.+GAM)                                               00430
0014              T12(GAM)=2.*GAM/(1.+GAM)                                                  00440
0015              T23(GAM)=2./(1.+GAM)                                                      00450
            C  DESCRIPTION OF INPUT                                                         00460
0016         60   FORMAT (4F10.0/5F10.0,3I4/3F10.0,3I4,/8F10.0)                             00500
0017         70   FORMAT ('1INPUT  A, B, C, SMA: ',3F10.1,F10.3/                            00510
                 1' DELTA, TWON, XZERO, BETA, BETA2, ITEST, PLAS, PRINT:',5F10.3,3I4        00520
                 2    / ' Z1, ZZERO, TOL, NUMINC, TM, TE: ',3F10.4,3I4, /                   00530
                 3      ' WIDTH, WAVEL, APER (1-3), WEIGHT(1-3): '8F10.4)                   00540
            C  IF TE=1  THEN  GAMMA=COS(ALPHA)/(N*COS(PHI))                                 00550
            C   APERATURES MUST BE INCREASING IN ABSOLUTE VALUE
            C  INITIALIZE                                                                   00560
```

```
      DATA DUMMY/C./, ELEC/'TE  '/, MAG/'TM  '/
      MXSLCT=3
      M=50
      LIMINC=4000
      NUMINC=50
      PI=3.141593
      INPER=0
      IS=0
      BETA2=0.
C     CONSTANTS FOR CALCULATING ADJUSTMENTS FOR PLASMA
      DELST1=.04
      DELST2=.1
      DELST3=.4
      DENS1=.20385E10
      DENS2=.69615E9
      DENS3=.11473E9
      DENS4=.22232E9
      GO TO 101
C   READ AND PRINT INPUT DATA
C WHEN BETA2=0 THEN XO PLANE IS TAKEN PERPENDICULAR TO X AXIS.
C    IF NO VALUE IS READ IN FOR BETA2, THEN IT CONTAINS ZERO.
  100 BETA2=0.
      YU=0.
      YL=0.
      XU=0.
      XL=0.
      Y=0.
      SUMW=0.
      DO 75 I=1,NSLCT
      J=I+MXSLCT
      W=WEIGHT(I)
      SUMW=SUMW+W
      YU=YU+SUMY(I)*W
      YL=YL+SUMY(J)*W
      XU=XU+SUMX(I)*W
      XL=XL+SUMX(J)*W
   75 Y=Y+AREA(I)*W
```

```
0051          Y=Y/SUMW
0052          IF (YU+XU) 77,76,77
0053    76    XU=1.
0054    77    PSIU=ARSIN(YU/SQRT(YU*YU+XU*XU))
0055          IF (YL+XL) 82,81,82
0056    81    XL=1.
0057    82    PSIL=ARSIN(YL/SQRT(YL*YL+XL*XL))
0058          X=PSIL-PSIU
0059          IF (ABS(X)-1.) 83,83,89
0060    89    WRITE (6,88) X
0061    88    FORMAT ('-ARCSIN ARGUMENT (PSIL-PSIU) ',E14.6,
             2  ' HAD ABSOLUTE VALUE GREATER THAN 1.','/'    SO POINTING ERROR' ,
             3      ' COULD NOT BE COMPUTED')
0062          INPER=INPER+1
0063          GO TO 95
0064    83    AL=ARSIN(X)/(2.*FACTK*Y)
0065          WRITE (6,80) AL,BETAP,BETA2P
0066    80    FORMAT ('-* * *'/6X,'POINTING ERROR IN RADIANS: ',E20.6,
             2  '   FOR PLANE ANGLES',2(4X,F6.3), ' DEGREES'/' * * *')
0067    95    IF(INPER-3) 101,990,990                                      00970
0068   101    READ (5,60,END=992,ERR=994) A,B,C,SMA,                        00980
             2     DELTA,TWON,XZERO,BETA,BETA2,ITEST,IPLAS,NPRINT,          00990
             3     Z1,ZZERO,TOL,NUMINC,TM,TE,                               00995
             4     WIDTH,WAVEL,(APER(I),I=1,3),(WEIGHT(I),I=1,3)            01000
0069          WRITE (6,70) A,B,C,SMA,                                       01010
             1     DELTA,TWON,XZERO,BETA,BETA2,ITEST,IPLAS,NPRINT,          01110
             3     Z1,ZZERO,TOL,NUMINC,TM,TE,                               01115
             4     WIDTH,WAVEL,(APER(I),I=1,3),(WEIGHT(I),I=1,3)            01120
0070          LIM=2*MXSLCT
0071          DO 102 I=1,LIM
0072          SUMX(I)=0.                                                    01140
0073   102    SUMY(I)=0.                                                    01150
0074          IS=0                                                          01160
0075          IERR=0                                                        01170
0076          IOUTP=0                                                       01180
0077          IVERT=0
0078          LVERT=0                                                       01190
0079          N=TWON                                                        01200
0080          ZZERO=ABS(ZZERO)                                              01210
```

```
0081              AE2=A-SMA
             C  CHECK INPUTS FOR VALIDITY
0082              IF (APER(1)) 1039,1039,103
0083         1039 WRITE (6,1038) (APER(I),I=1,MXSLOT)
0084         1038 FORMAT ('0THE FIRST APERATURE (CENTER) VALUE MUST BE'
                2  ' GREATER THAN ZERO AND ANY REMAINING VALUES MUST '
                3  'FOLLOW IN ORDER OF INCREASING MAGNITUDE',3E20.6)
0085              GO TO 199
0086          103 NSLOT=1
0087              DO 104 I=2,MXSLOT
0088              IF (APER(I)) 1039,106,105
0089          105 IF (APER(I)-APER(I-1)) 1039,1039,104
0090          104 NSLOT=I
0091          106 IF (TWCN-1.) 109,110,110
0092          109 WRITE (6,108)
0093          108 FORMAT (' VALUE FOR REFRACTIVE INDEX N IS LESS THAN OR = 1.')
0094          199 WRITE (6,198)
0095          198 FORMAT (' DATA SET IS NOT USED')
0096              INPER=INPER+1
0097              GO TO 95
             C
0098          110 IF (NUMINC) 114,114,112
0099          112 IF (NUMINC-LIMINC) 120,120,114
0100          114 NUMINC=LIMINC
0101              WRITE (6,113) NUMINC
0102          113 FORMAT (' VALUE FOR THE LIMIT OF THE NUMBER OF INCREM'
                1'ENTS IS UNREASONABLE, ASSUMED VALUE ', I4)
             C
0103          120 IF (BETA) 119,124,121
0104          121 IF (BETA-55.   ) 124,124,119
0105          119 WRITE (6,118)
0106          118 FORMAT (  ' VALUE FOR BETA OR BETA2 IS NOT BETWEEN ZERO',
                1  14HAND 55 DEGREES )
0107              GO TO 199
             C
```

```
124   IF (BETA2) 119,130,125
125   IF (BETA2-55.) 130,130,119
C
130   IF (Z1) 140,131,129
131   WRITE (6,127)
127   FORMAT ('THE INPUTTED VALUE 0 FOR Z1 IS INVALID')
      GO TO 199
129   WRITE (6,128)
128   FORMAT (' NEGATIVE OF GIVEN VALUE FOR Z1 IS ASSUMED')
      Z1=-Z1
C
140   IF (DELTA) 1409,1409,141
141   IF(DELTA+(Z1/2.))  144,144,1409
1409  WRITE (6,1408)
1408  FORMAT (' VALUE FOR DELTA IS UNREASONABLE')
      GO TO 199
C
144   IF (C) 146,145,146
145   VERTF1=A
      VERTF2=AF2

      GO TO 152
146   IF (AF2-C) 1469,150,150
1469  WRITE (6,1468)
      GO TO 199
1468  FORMAT (' POSITION OF FUNCTION DOES NOT GIVE PROPER SHAPE',
     1'--A NEW A,B,C ARE NEEDED.')
150   VERTF1=B-SQRT(A*A-C*C)
      VERTF2=B-SQRT(AF2*AF2-C*C)
152   WRITE (6,151) VERTF1,VERTF2
151   FORMAT (5X,4(2X,E13.6))
C
      IF (XZERO-VERTF2) 1509,1509,156
156   IF (VERTF1) 1569,1569,154
1569  WRITE (6,1568) VERTF1
1568  FORMAT (' VERTEX OF F1 SHOULD BE RIGHT OF ZERO BUT IS AT ',F10.3)
      GO TO 199
C
```

```
  154 IF (BETA2) 161,160,161
C                                                                        01990
  160 UF2X0=FX(+1,AF2,B,C,XZERO)
      BF2X0=-UF2X0                                                       02010
      XUP=XZERO                                                          02020
      XLO=XZERO                                                          02030
      XIM=XZERO                                                          02040
      GO TO 163                                                          02050
  161 MX0=-1./TAN(BETA2*PI/180.)
      CALL XPT(+1,MX0,XZERO,0.,AF2,B,C,XUP,UF2X0,IERR)
      CALL XPT(-1,MX0,XZERO,0.,AF2,B,C,XLO,BF2X0,IERR)                   02070
        XLO=XZERO+ZZERO*SIN(BETA2*PI/180.)
  163 F2X0=UF2X0                                                         02080
      WRITE (6,151) XLO,BF2X0,XUP,UF2X0
      COSBE=COS (BETA2*PI/180.)
      IF (ZZERO*COSBE-F2X0) 157,157,1639
 1639 ZZERO=ABS(F2X0)/COSBE-10.E-6
      WRITE (6,1638) ZZERO                                               02110
 1638 FORMAT ('0VALUE FOR ZZERO DOES NOT LIE WITHIN REGION 3'/           02120
     1' VALUE FOR F2(X0)IS ASSUMED',F10.6)                               02130
  157 IF (BETA)  155,164,155
  155 S=-1./TAN(BETA*PI/180.)
      IERR=2
      CALL XPT(-1,S  ,0.,0.,A,B,C,X,Y,IERR)
      IF (IERR) 164,158 ,164
  158 IF (Y) 159,159,164
  159 IF (X-XLO) 1589,1589,164
 1589 WRITE (6,1588) X,Y                                                 01960
 1588 FORMAT (' INCIDENT PLANE INTERSECTS FUNCTION AT ',2E9.2)           01970
      GO TO 199                                                          01980
C  TEST IF X0 PLANE IS TOO FAR RIGHT                                     01850
  164 IF (C) 153,167,153
  153 IF (B-XLO) 1509,1509,167
 1509 WRITE (6,1508)                                                     01820
 1508 FORMAT (' RECEIVING PLANE IS TOO FAR RIGHT')                       01830
      GO TO 199                                                          01840
C  THIS IS END OF INPUT DATA CHECKING ROUTINES                           02140
C                                                                        02150
```

```
C  CONVERT DATA INTO PROPER UNITS FOR CALCULATIONS
 167  BETAP=BETA
      BETA=BETA*PI/180.
      ABM=TAN(BETA)
      FACTK=2.*PI/WAVEL
      DK=FACTK*WIDTH
      BETA2P=BETA2
      ZZERO=ZZERO*COSBE
      WIDTH=WIDTH*COSBE
      DO 168 I=1,3
 168  APER(I)=APER(I)*COSBE
      GN=TWON
      CASE=MAG
      IF (TM-1) 165,170,170
 165  IF (TE-1) 170,166,170
 166  GN=1./TWON
      CASE=ELEC
 170  WRITE (6,171)
 171  FORMAT ('1VALID INPUT DATA IS READY--COMPUTATIONS BEGIN',
     1   ' (FOR QUADRATIC CASE)'/)
      WRITE (6,173)  BETAP,BETA2,XZERO,N,DELTA,CASE
 173  FORMAT ('    BETA=',F6.2,3X,'BETA2=',F6.2,
     1                        7X,'XO=',F6.2,7X,'N=',F5.2,7X,
     1'DELTA=',F6.3,7X,'CASE=',A4)
      WRITE (6,175)
 175  FORMAT (1H-,33X,'FINAL INTERCEPT'/
     1 'INCREMENT',2X,'STARTING POINT',3X,'RAY',5X,'X',7X,'Z',
     2  5X,'AMPLITUDE',3X,'DISTANCE',9X,'ANGLE')
      ZEM=Z1
      IHIT=0
      KHITSL=0
      GO TO 206
C
```

```
     C   INCREMENT FOR EMANATING POINT ON WAVE FRONT
0198     180  WRITE (6,178)        XM,XEM,ZEM,A,B,C, ICALL
0199     178  FORMAT (' NEGATIVE DISCRIMINANT ',
            1' WAS OBTAINED IN SUBROUTINE XPT WITH ARGUMENTS ',
            2 2(/3(3X,F17.6)),I4)
0200     200  ZEM=ZEM+DELTA*COS(BETA)
0201          IF (KHITSL) 204,204,203
0202     203  IF (IS) 2039,2039,204
0203     2039  WRITE (6,2038)
0204     2038 FORMAT (' WARNING: FIRST RAY DID NOT PASS BELOW ZO'
            1' ON XZERO PLANE')
0205     204  IS=IS+1
0206          IF (NUMINC-IS) 2049,206,206
0207     2049 WRITE (6,2048) NUMINC
0208     2048 FORMAT ('-SPECIFIED NUMBER OF INCREMENTS ARE MADE',I4)
0209          GO TO 100
0210     206  IBELO=0
     C * * * * *    BEGIN CALCULATIONS
0211          IHOT=0
0212          INOP=0
0213          IPROC=0
0214          ALPHA=0.

0215          PHI=0.
0216          GAMMA=0.
0217          TC=0.
0218          DISTC=0.
0219          PHI2=0.
0220          BCM=0.
0221          BMN=0.
0222          XEM=-ZEM*ABM
     C
0223     210  IF (ITEST) 212,216,212
0224     212  WRITE (6,1212) IS,XEM,ZEM
0225     1212 FORMAT (1H2,I3,'TH INCREMENT HAS BEEN ADDED TO STARTING POINT'
            1/' RAY ORIGINATES FROM POINT: '2F14.7)
0226     214  IF (ZEM) 216,215,2149
```

```
      2149 WRITE (6,2148) IS                                                    02860
      2148 FORMAT (1H ,I4,'TH INCREMENT ON Z1 HAS REACHED X AXIS')              02870
    C  FIND WHERE RAY INTERSECTS F1, (XP, ZB)                                   02890
           GO TO 217                                                            02900
      216  ISIGN=-1                                                             02910
           IF (ABM) 2160,2165,2160                                              02920
      2160 IF ((XEM-ZEM/ABM)-VERTF1) 217,2161,218                               02930
      2161 LVERT=1                                                              02940
           GO TO 2339                                                           02950
      2165 IF (ZEM) 218,2161,217                                                02960
      217  ISIGN=+1                                                             02970
           IBELC=2
           IF (IVEPT-1) 2170,218,2170
      2170 LVERT=1                                                              02990
           IVERT=1
           WRITE (6,2169) IS,LVERT                                              03000
      2169 FORMAT ('ORAY' ,I5,' PASSED LEFT OF VERTEX OF F',I2)                 03010
      218  CALL XPT(ISIGN,ABM,XEM,ZEM,A,B,C,XB,ZB,IBELO)                        03020
           ICALL=1                                                              03030
    C  IF LINE DID NOT INTERSECT WITH F THEN A NON-OVALUE IS                    03040
    C      RETURNED IN IBELO                                                    03050
           IF (IBELC) 219,1219,219
    C (NOTE: NOT CORRECT IF ALPHA IS NEGATIVE-I.E.WHEN REFLECTIONS GO TOWARDS V03110
    C       VERTEX                                                              03115
      219  IF (IHIT) 200,200,700                                                03120
      1219 IF (ZB*ISIGN) 700,220,220
    C CHECK IF RAY CROSSED XC PLANE                                             03130
      220  IF (ISIGN) 221,221,222                                               03140
      221  IF (XLC-XB) 200,200,224                                              03150
      222  IF (XUP-XB) 700,700,224                                              03160
    C                                                                           03170
    C  FIND ALPHA (ANGLE OF INCIDENCE)                                          03180
      224  BMN=-1./FDERX(ISIGN,A,B,XB)                                          03190
           IF (IPLAS) 223,225,223
      223  IF (IHOT) 230,225,230
     225   ALPHA=(-ISIGN)*(ATAN(BMN)-BETA)                                      03210
           PHI1=ARSIN (SIN(ALPHA) /N)                                           03220
           GAMMA=GN*COS(ALPHA)/COS(PHI1)                                        03230
           DISTO=FDIST(XEM,XB,ZEM,ZB)                                           03240
           TC=2.*GAMMA/(1.+GAMMA)                                               03260
    C      MAKE ADJUSTMENTS FOR PLASMA          PPPPPPPPPPPPPPPPPPPP
```

```
0259            IF (IPLAS) 1220,226,1220
0260      1220 IF (XB) 10C,1222,1222                                           P
0261      1222 CONST=DELST1*DENS1                                              P
0262            IF (XB-5.) 1240,1240,1224                                      P
0263      1224 CONST=DELST1*DENS2                                              P
0264            IF (XB-10.) 1240,124C,1226                                     P
0265      1226 CONST=DELST2*DENS3                                              P
0266            IF (XB-15.) 1240,1240,1228                                     P
0267      1228 CONST=DENS3                                                     P
0268            IF (XB-20.) 1236,1236,1230                                     P
0269      1230 CONST=DENS4                                                     P
0270            IF (XB-48.) 1236,1236,100                                      P
0271      1236 CONST=CONST*DELST3                                              P
0272      1240 X=TAN(ALPHA)                                                    P
0273            Y=1./COS(ALPHA)                                                P
0274            U=(1.61E-12)*Y*CONST                                           P
0275            DELX=U*X*Y                                                     P
0276            DPLAS=U*(1.-X*X)                                               P
          C   CONICAL CASE PLASMA-ADJUSTMENT FOR X COORDINATE:
0277            DX=FDERX(ISIGN,A,B,XB)
0278            XB=XB+DELX*(COS(ABS(ATAN(DX))))
0279            DX=FDERX(ISIGN,A,B,XB)                                         8
0280            ZB=FX(ISIGN,A,B,C,XB)
0281            DISTO=DISTO+DPLAS
0282            IHOT=1                                                         P
          C     END OF PLASMA CALCULATIONS                                     P
0283      226   IOUTP=0                                                            03270
0284            IW=0                                                               03280
0285            IHIT=1                                                             03290
0286            KLOOP=0
0287            IF (IPLAS) 220,230,220                                             03295
          C   ENTER MAIN LOOP HERE -- AFTER EITHER (AT LEAST)  * * * * * * * * *   03310
          C      TWO REFLECTIONS INREGION 2 OR RAY HAS FIRST PASSED                03320
          C      FROM REGION 1 TO REGION 2.                                        03330
          C   FIND COORDINATES OF POINT C (WHICH IS ON BORDER REGIONS 2,3)         03340
          C   FIND SLOPE OF LINE FROM B TO C                                       03350
```

```
  230 BCM=TAN(ATAN(BMN)+ISIGN*PHI1)
      KLOOP=KLOOP+1
      IF (KLOOP-50) 231,9231,9231
 9231 WRITE (6,8231) KLOOP
 8231 FORMAT (' LOOP BEGINNING STMT NO. 230 HAS BEEN PERFORMED ',
     1 I4, ' TIMES--RAY IS IGNORED')
      INPER=INPER+1
      GO TO 100
  231 IF (BCM*ISIGN) 232,1235,1234
  232 IF ((XB-ZB/BCM)-VERTF2) 233,2329,1235
 2329 LVERT=2
 2339 WRITE (6,2338) IS,LVERT
 2338 FORMAT ('ORAY',I5,' HIT DIRECTLY ON POINT AT SURFACE',
     1 I2,'; SO RAY WAS IGNORED')
      GO TO 200
  233 ISIGN=-ISIGN
      LVERT =2
      WRITE (6,2169) IS,LVERT
 1234 IBELO=2
 1235 CALL XPT (ISIGN,BCM,XB,ZB,AF2,B,C,XC,ZC,IBELO)
      IF (IBELO) 800,239,800
C CHECK IF RAY CROSSED XO PLANE
  239 XX=XLO
      IF (ISIGN) 236, 236, 235
  235 XX=XUP
  236 IF (XX-XC) 480,480,237
C  CALCULATE DISTANCE TO C
  237 IF (ZC*ISIGN) 800,238,238
  238 BC=FDIST(XB,XC,ZB,ZC)
      DISTO=DISTO+BC*N
C  FIND SLOPE OF NORMAL FROM POINT C (ON F2)
  240 CMN=-1./FDEFX(ISIGN,AF2,B,XC)
C  CALCULATE SLOPE OF LINE FROM C THRU REGION 3 TO X=XO PLANE
      PHI2=ISIGN*(ATAN(BCM)-ATAN(CMN))
```

```
0316          SINP2=SIN(PHI2)                                                       03860
0317          IF (N*SINP2-1.) 241,9241,9241                                         03870
0318     9241 IF (NPRINT) 200,7241,200
0319     7241 WRITE (6,8241) IS,XEM,ZEM
0320     8241 FORMAT (1H-,3X,I5,4X,'(',F6.3,1X,F7.3,')',2X,                         03890
         1 ' RAY WAS NOT TRANSMITTED TO THIRD MEDIUM AFTER REACHING IT')            03900
0321          GO TO 200                                                             03910
0322      241 ALPHC=ARSIN(N*SIN(PHI2))                                              03920
0323          X=     (ATAN(CMN)+ISIGN*ALPHC)                                        03930
0324          IT=1
0325          CALL TUN(X,IT)
0326          IF (IT) 245, 95,245
0327      245 CZM=X
0328          GAMMA=GN*COS(ALPHC)/COS(PHI2)                                         03940
0329          T2= 2./(1.+GAMMA)                                                     03950
0330          RTEMP=R22(GAMMA)                                                      03960
0331          IF (ABS(TO*T2)-TOL) 480,480,243
0332      243 IOUTP=IOUTP+1                                                         03970
0333          KLP2=0
        C  CALCULATE Z COORD OF POINT ON XZERO PLANE                                03980
0334          IF (BETA2) 244,242,244                                                03990
0335      242 Z(IOUTP)=ZC+CZM*(XZERO-XC)                                            04000
0336          GO TO 246                                                             04010
0337      244 XIM=(MXO*XZERO+ZC-CZM*XC)/(MXO-CZM)                                   04020
0338          Z(IOUTP)=MXO*(XIM-XZERO)                                              04030
0339      246 IF (ITEST-1) 250,2509,2509                                            04040
0340     2509 WRITE (6,2508) ISIGN,Z(IOUTP)                                         04050
0341     2508 FORMAT (1X,I4,E13.6)                                                  04060
        C  TEST WHETHER RAY FALLS ON XZERO PLANE WITHIN REGION 3                     04070
0342      250 IRR=1                                                                 04080
0343          ABSZ=ABS(Z(IOUTP))
0344          IF (ABS(ZZERO)-ABSZ)  260,400,400
        C  IRELO= 1 MEANS RAY PASSED BELOW NEGATIVE Z0 LIMIT.                        04100
0345      260 IF(Z(IOUTP))270,400,280                                               04110
0346      270 IF (ABS(FF2XC)-ABSZ)  300,290,290
0347      280 IF(ABS(LF2X0)-Z(IOUTP))300,290,290                                    04140
0348      290 IRELO=SIGN(1.,Z(IOUTP))
0349          GO TO 480
        C  STORE INFORMATION FOR LATER CALCULATION OF RAYS REFLECTING IN REGION     S4180
0350      300  INCP=INCP+1
```

```
      IF(INOP-M)340,320,309                                            S4200
  309 WRITE(6,308)                                                     S4210
  308 FORMAT ('-**** REFLECTION STORAGE EXCEEDED,',                    S4220
     U ' FINAL OUTPUT MAY NOT HAVE COMPLETE SET OF POINTS')            S4230
      INOP=INOP-1                                                      S4240
      GO TO 350                                                        S4250
  320 WRITE(6,318)                                                     S4260
  318 FORMAT('0**WARNING: REFLECTION STORAGE FILLED, PROGRAM MAY NEED TO S4270
     1 BE RECOMPILED WITH A LARGER M')                                 S4280
  340 SX(INOP)=XC                                                      S4290
      SZ(INOP)=ZC                                                      S4300
      SM(INOP)=CMN                                                     S4310
      SPHI(INOP)=PHI2                                                  S4320
      SD(INOP)=DISTO                                                   S4330
      ST(INOP)=TO                                                      S4340
      SR(INOP)=RTEMP                                                   S4350
C     BEGIN LOOP FOR RAY BOUNCING BACK AND FORTH IN REGION 3           S4360
C     ISIGN INDICATES THE SIGN OF THE F2 THAT THE RAY IS DIRECTED TOWARD S4370
C                                 (TO THE TOP OR BOTTOM OF WEDGE)      S4380
  350 ISIGN=SIGN(1.,CZM)
      CALL XPT(ISIGN,CZM,XC,ZC,AF2,B,C,XF,ZE,IERR)                     04400
      IF (IERR) 359,360,359                                            04410
  359 ISTAT=359
      WRITE (6,358) ISTAT,IERR,ISIGN,CZM,XC,ZC,AF2,B,C,XE,ZE
  358 FORMAT ('OGADS: NO INTERSECTION--SEE STATEMENT ' ,I4,
     1 /4X,2I4,8F14.5)
      GO TO 95                                                         04450
  360  XX=XLO
      IF (ISIGN) 362,362,361
  361 XX=XUP
  362 IF (XX-XF) 480,480,365
  365 EMN=-1./FDERX(ISIGN,AF2,B,XF)
      ALPHA=PI+ISIGN*(ATAN(EMN)-ATAN(CZM))                             04470
      PHI2=ARSIN(SIN(ALPHA)/N)                                         04480
      TC=TO*T2                                                         04490
```

```
      GAMMA=GN*CCS(ALPHA)/COS(PHI2)                                      04500
      T2=R33(GAMMA)                                                      04510
      RTEMP=2.*GAMMA/(1.+GAMMA)                                          04520
      DISTO=DISTO+FDIST(XC,XE,ZC,ZE)                                     04530
      IF (ABS(TO*T2)-TOL)  480,370,370                                   04540
  370 X=      (ATAN(EMN)+ISIGN*ALPHA)                                    04550
      IT=2
      CALL TUN(X,IT)
      IF (IT) 373, 95,373
  373 EZM=X
      IF (BETA2) 372,371,372                                             04560
  371 Z(IOUTP)=ZE+EZM*(XZERO-XE)                                         04570
      GO TO 374                                                          04580
  372 XIM=(MXO*XZERO+ZE-EZM*XE)/(MXO-EZM)                                04590
      Z(IOUTP)=MXO*(XIM-XZERO)                                           04600
  374 IF (ITEST) 369,376,369
  369 WRITE (6,448) ISIGN,EMN,XC,ZC,CMN,ALPHA, PHI1,GAMMA,T2,
     1     DISTO,TO,CZM,XE,ZE,PHI2,ALPHC,EZM
  376 XC=XE                                                              04630
      ZC=ZE                                                              04640
      CZM=EZM                                                            04650
      CMN=EMN                                                            04660
      IBELO=0                                                            04670
      KLP2=KLP2+1
      IF (KLP2-10) 250,399,399
  398  FORMAT ('0 LOOP STMT 390.')
  399 WRITE (6,398)  KLP2
      GO TO 200
  400 ANGLE(IOUTP)= BETA2-ATAN(CZM)*180./PI                              04740
      AMPL(IOUTP)=TO*T2                                                  04750
  404 IF (ABS(AMPL(IOUTP))-TOL)  480,406,406                             04760
  406 DIST(IOUTP)=DISTO+FDIST(XIM  ,XC,Z(IOUTP),ZC)                      04770
C  RESULTS ARE NOT PRINTED IF RAY PASSED ABOVE OR BELOW ZO LIMITS        04780
C  HOWEVER, FURTHER CALCS ARE MADE SINCE THERE IS POSSIBILITY            04790
C      THAT REFLECTIONS WILL FALL WITHIN LIMITS.                         04800
```

```
      ISLOT=0
      ABSZ=ABS(Z(IOUTP))
      DO 415 I=1,MXSLOT
      IF (ABS(APER(I))-WIDTH-ABSZ) 410,440,440
  410 IF (ABS(APER(I))+WIDTH-ABSZ) 415,415,412
  412 ISLOT=I
      CENTR=APER(I)
      IF (Z(IOUTP)) 414,420,420
  414 ISLOT=ISLOT+MXSLOT
      CENTR=-CENTR
      GO TO 420
  415 CONTINUE
      GO TO 440
  420 ANG=ANGLE(IOUTP)*PI/180.
      DAMP=COS((PI*COSBE/(2.*WIDTH))* (Z(IOUTP)-CENTR)/COSBE)
      AMPL(IOUTP)=AMPL(IOUTP)*DAMP*DAMP
      POLR=AP(ANG,AMPL(IOUTP))
      POLTH=DIST(IOUTP)*FACTK
      RECTX=POLR*COS(POLTH)
      RECTY=POLR*SIN(POLTH)
      SUMX(ISLOT)=SUMX(ISLOT)+RECTX
      SUMY(ISLOT)=SUMY(ISLOT)+RECTY
      ALPHAP=ALPHA*180./PI
      IW=IW+1
      KHITSL=KHITSL+1
      IF (KHITSL-1) 421,422,421
  421 IF (NPRINT) 440,422,440
  422 IF (IW    -1) 434,424,434
  424 WRITE (6,426) IS,XEM,ZEM,IOUTP,XIM,Z(IOUTP),AMPL(IOUTP),
     1       DIST(IOUTP),ANGLE(IOUTP)
  426 FORMAT (1H-,2X,I4,4X,'(',F6.3,1X,F7.3,')',2X,I2,3X,F7.4,
     1   1X,F7.4,2X,F9.6,3X,F13.6,4X,F9.5)
      GO TO 440
  434 WRITE (6,436) IOUTP,XIM,Z(IOUTP),
     1             AMPL(IOUTP),DIST(IOUTP),ANGLE(IOUTP)
  436 FORMAT (1H ,28X,I2,3X,F7.4,
     1   1X,F7.4,2X,F9.6,3X,E13.6,4X,F9.5)
  440 AMPLT=T0*T2*RTEMP*R22(GAMMA)
CCC   IF (AMPL(IOUTP)-AMPLT) 449,449,444
  444 IF (ITEST) 449,450,449
```

```
0446     449  WRITE (6,448) ISIGN,ABM,XB,ZB,BMN,ALPHA,PHI1,GAMMA,T2,
             1    DISTO,TO,BCM,XC,ZC,PHI2,ALPHC,CZM
0447     448  FORMAT (I4,5(2X,4F15.6/))
0448     450  IF (IOUTP-29)500,470,479
0449     470  WRITE (6,472)
0450     472  FORMAT (' WARNING: PROGRAM LIMIT OF 29 PAIRS OF REFLE'
             1'CTIONS'/' (IN REGION 2)-PER EACH ORIGINAL RAY--',
             2'HAS BEEN REACHED')
0451          GO TO 500
0452     479  WRITE (6,478) AMPLT
0453     478  FORMAT (' PROGRAM LIMIT OF NO. OF REFLECTIONS',
             1' FOR RAY HAS BEEN EXCEEDED',
             1/' WITH AMPLITUDE OF ABOUT ',E13.6)
0454          GO TO 200
        C * * * * * * *
        C     PROCESS RAYS FROM ANY REMAINING REFLECTION POINTS
0455     480  IF (INOP) 200,200,490
0456     490  IF (IPROC-INOP) 494,200,200
0457     494  IPROC=IPROC+1
0458          IOUTP=0
0459          XC=SX(IPROC)
0460          ZC=SZ(IPROC)
0461          CMN=SM(IPROC)
0462          PHI2=SPHI(IPROC)
0463          DISTO=SD(IPROC)
0464          TO=ST(IPROC)
0465          RTEMP=SR(IPROC)
        C* * * * *
        C  CALCULATE  ITEMS FOR REFLECTION FROM POINT C TO D  (IN REGION 2)
        C           THEN  REENTER LOOP
0466     500  ISIGN=SIGN(FLOAT(ISIGN),ZC)
0467          X=      (ATAN(CMN)-ISIGN*PHI2)
0468          IT=3
0469          CALL TUN(X,IT)
0470          IF (IT) 502, 95,502
0471     502  CDM=X
```

```
      CALL XPT(ISIGN,CDM,XC,ZC,A,B,C,XD,ZD,IERR)
      ICALL=3
      IF (IERR) 180,504,180
  504 XX=XLO
      IF (ISIGN) 510,510,505
  505 XX=XUP
  510 IF (XX    -XD) 480,480,520
  520 DMN=-1./FDERX(ISIGN,A,B,XD)
      PHI3=ISIGN*(ATAN(DMN)-ATAN(CDM))
      IF (CDM*ISIGN) 540,540,530
  530 PHI3=PI+PHI3
  540 SINP3=SIN(PHI3)
      IF (SINP3)549,549,542
  549 WRITE (6,548)
  548 FORMAT (' PHI IS NEGATIVE (EEK)')
      WRITE (6,448) ISIGN,PHI3,XC,ZC,XD,ZD,CDM,DMN,XB,ZB
      GO TO 100
  542 IF (TWON*SINP3-1.) 545,580,580
  545 ALPHA=ARSIN(TWON*SINP3)
      GAMMA=  GN*COS(ALPHA)/COS(PHI3)
      TO=TO*PTEMP*R22(GAMMA)
  555 IF (ABS(TO)-TOL)  480,480,550
  550 DISTO=DISTO+FDIST(XC,XD,ZC,ZD)*T,WON
      PHI1=PHI3
      BMN=DMN
      XB=XD
      ZB=ZD
      IF (ITEST) 560,230,560
  560 WRITE (6,448) ISIGN,ABM,XB,ZB,BMN,ALPHA,PHI1,GAMMA,T2,
     1   DISTO,TC,BCM,XC,ZC,PHI2,ALPHC,CZM
      GO TO 230
C  WHEN RAY IS NOT TRANSMITTED INTO REGION 1 FROM REGION 2 BUT REFLECTS
C     ONLY.
  580 Y=N*SQRT(N*N*SINP3*SINP3-1.)
```

```
      DISTO=DISTO+2.*ATAN(Y)
C     AMPLITUDE IS UNCHANGED
      TO=TO*RTEMP*1.
      GO TO 555
C
C        WHEN RAY PASSES ABOVE +F1
  700 WRITE (6,710) IS
  710 FORMAT ('-RAY PASSED ABOVE FUNCTION * * * '/
     1        '0* THIS COMPLETES PROCESSING OF DATA SET'/
     2        ' * ',I5,' INCREMENTS HAVE BEEN ADDED TO Z1')
      GO TO 100
C     WHEN RAY PASSES ABOVE  +F2 OR BELOW -F2
  800 IBELO=0
      IF (ISIGN*BCM) 480,480,802
  802 CALL XPT(ISIGN,BCM,XB,ZB,A,B,C,XD,ZD,IBELO)
      IF (IBELO) 480,805,480
  805 CDM=BCM
       XC=XB
      ZC=ZB
      RTEMP=1.
      GO TO 504
  900 WRITE (6,910)  BCM,XB,ZB,XD,ZD,IBELO
  910 FORMAT (' DOES IT MATTER?',5F14.6,I2)
      GO TO 200
C* * * * *
C   EXITS FROM PROGRAM
  990 WRITE (6,991) INPER
  991 FORMAT (I2,' INPUT ERRORS RESULTED IN PROGRAM END')
      GO TO 999
  994 WRITE (6,995)
  995 FORMAT (' ERROR OCURRED DURING READ')
      GO TO 999
  992 WRITE (6,9929)
 9929 FORMAT (' ALL DATA HAS BEEN PROCESSED')
  999 STOP
      END
```

TOTAL MEMORY REQUIREMENTS 0048CA BYTES

```
      SUBROUTINE TUN(X,IX)
      INTEGER LIST(2)/1,259/
      CALL GETIHC(IERR,LIST,&99)
      X=TAN(X)
      CALL PUTIHC
      RETURN
   99 WRITE (6,98) X,IX
      CALL PUTIHC
      IX=0
      RETURN
   98 FORMAT ('0COMPUTATION FOR DATA SET IS TERMINATED '
     2'BECAUSE TANGENT ARGUMENT ',E14.6,
     3' IS TOO CLOSE TO SINGULARITY FOR FORTRAN ROUTINES (',I1,')'
     4/' SUGGEST THAT FIRST STARTING POINT (Z1) BE MOVED SLIGHTLY.')
      END
```

TOTAL MEMORY REQUIREMENTS 00029E BYTES

```
      SUBROUTINE XPT(ISIGN,SLM,SLX,SLZ,A,B,C,X,Z,IERR)
C  SUBROUTINE TO FIND WHERE A GIVEN STRAIGHT LINE (SL)
C     INTERSECTS F1 OR F2, WHICH ARE SEGMENTS OF CONCENTRIC CIRCLES
C        WITH RADIUS A AND CENTER (B,C).
C     INPUT IS SLOPE AND A POINT OF LINE,
C        AND COEFFICIENTS OF F1 OR F2.
C     OUTPUT IS X AND Z COORDINATES OF INTERSECTION POINT.
C        AND ERROR INDICATOR WHICH WILL=0 WHEN
C        A REAL VALUED INTERSECTION POINT HAS BEEN OBTAINED
C     ISIGN= -1  INDICATES UPPER CIRCLE,
C        I.E., THE PART OF F1 OR F2 WHICH IS IN 4TH QUADRANT.
C     THE BOTTOM POINT IS SOVED FOR EXCEPT WHEN IERR=2(=IPT).
C     ISIGN= +1 INDICATES LOWER CIRCLE,
C        I.E., THE PART OF F1 OR F2 WHICH IS IN FIRST QUADRANT.
C     THE TOP   POINT IS SOLVED FOR EXCEPT WHEN IERR=2(=IPT).
C     IPT=2 ONLY WHEN RAY PASSES LEFT OF VERTEX OF EITHER F1 OR F2.
```

```
      CTHER=1
      IPT=IERR
      IF (IPT-2) 5,3,5
    3 CTHER=-1
    5 IERR=0
      ASL=-SLM
      IF (ASL) 7,6,7
C  LINE IS HORIZONTAL
    6 Z=SLZ
      AQ=1.
      BQ=-B-B
      CQ=Z*(Z+ISIGN*(C+C))+B*B+C*C-A*A
      DISCR = BQ*BQ-4.*AQ*CQ
      IF (DISCR) 9,16,16
   16 X=-.5*(BQ+SQRT(DISCR))
      GO TO 14
    7 BSL=1.
      CSL=-(SLZ+SLX*ASL)
      AQ=BSL*BSL+ASL*ASL
      BQ=2.*(BSL*CSL+ISIGN*ASL*ASL*C+B*BSL*ASL)
      CQ=CSL*CSL+2.*B*ASL*CSL-ASL*ASL*(A*A-B*B-C*C)
      DISCR = BQ*BQ-4.*AQ*CQ
      IF (DISCR) 9,10,10
    9 IERR=1
      RETURN
   10 Z=(-BQ+ISIGN*CTHER*SQRT(DISCR))/(2.*AQ)
      X=-(BSL*Z+CSL)/ASL
C  F1 AND F2 HAVE RIGHT-HAND LIMIT OF X=B
   14 IF (B-X) 9,15,15
   15 RETURN
      END

   TOTAL MEMORY REQUIREMENTS 0004DA BYTES
EXECUTION TERMINATED
```

```
      SUBROUTINE XPT(ISIGN,M1,X1,Y1,X2,M2,Y2,X,Y,IERR)
C  THIS VERSION OF XPT IS TO BE USED IN THE CONICAL CASE
C  YIELS THE INTERSECTION POINT OF TWO STRAIGHT LINES
C     GIVEN THE SLOPES AND A POINT ON EACH.
      REAL M,M1,M2
      M=M2*ISIGN
      IF (M1-M) 10,9,10
    9 IERR=1
      RETURN
   10 IERR=0
      X=(M1*X1-M*X2+Y2-Y1)/(M1-M)
      Y=M1*(X-X1)+Y1
      RETURN
      END
```

(5) Variable List (partial)* for FORTRAN Computer Program with Meaning and Use**

ABM	Slope of ray from point A (where ray originates) to point B.
AF2	The A constant for function F2.
ALPHA	Angle between ray approaching F1 in Region I and slope of normal to F1 at intersection point B
ALPHC	Angle between ray leaving F2 in Region III and slope of normal to F2 at point C.
BC	Geometric distance between point B (on F1) and point C (on F2).
BCM	Slope of ray from point B to point C.
BETAP	The angle β, in degrees for printing purposes.
BETA2P	The angle $\beta 2$, in degrees for printing purposes.
BF2XO	Z-coordinate of the bottom intersection point that the receiving plane, centered at X_0, makes with the radome.
BMN	Slope of normal to F1 at point B.
CASE	Contains the literal 'MAG' when data for magnetic case is being processed and 'ELEC' for the electrical case; used in print-out.
CMN	Slope of normal F2 at poinc C.
COSBE	Result of cosine function applied to β.
CZM	Slope of ray transmitted at point C into Region III.
CAMP	Result of function which damps the amplitude.
DELX	Used in plasma calculations; represents the change in distance along the function F1.
DK	(2π/wavelength)*(width of slot).
DPLAS	The change in optical distance caused by presence of plasma.
DX	Used for results of taking derivatives.

* Input variables are included in another section

** See diagram in Section (2) for aid in understanding symbols used in the program.

Variable List (continued)

EMN	Slope of normal to F2 at a point E.
EZM	Slope of ray reflected at a point E in region towards receiving plane.
FACTK	2π/wavelength
GAMMA	The factor used to compute reflection and transmission coefficients.
GN	Contains the index of refraction during calculations for the magnetic polarization and its inverse for the electrical polarizations.
IBELO	Is argument of call to subroutine XPT. Indicates which point of intersection of surface with the circle is to be used (quadratic case).
IERR	Usually used in call to subroutine XPT, in which case value 0 means a satisfactory intersection was found.
IHIT	Registers 0 during computations for a data set until the first ray hits the radome.
IHOT	Registers 0 during computations for a data set until plasma adjustments are made (if any).
INOP	The count of the number of points in storage to be processed for reflections.
INPER	The count of the number of times input data errors have been detected.
IOUTP	The count of the number of output points.
IPROC	The count of the number of points in reflection storage that have been processed.
IS	The number of increments that have been added to the original starting point on incoming plane.
ISIGN	+ 1 when intersection with top function is being sought; - 1 for bottom part.
IVERT	Is set to 1 for remainder of data set computation when some originating ray first passes left of vertex of F1.
KHITSL	Indicator to allow printing of more information when the first component of a ray hits any slot.

Variable List (continued)

KLOOP	Count of the number of times for a particular ray that the main loop has been performed.
KLP2	Counts number of times a ray reflects wholly within Region III.
LIMINC	Program limit to the number of increments that can be made, i.e. the number of points used on incoming plane.
LVERT	Contains the number of vertices for which rays have passed to the left within a given data set (e.g. 0, 1, 2).
M	Contains number of points for which reflections storage is capable of holding information.
MXO	Slope of receiving plane, which is centered at $(X_o, 0)$.
MXSLOT	The maximum number of pairs of slots program can process.
PHI1	Angle in Region II between ray and normal to F1, outer surface.
PHI2	Angle in Region II between ray and normal to F2, inner surface.
PHI3	Angle in Region II between a reflected ray and the normal to F1, outer surface.
POLR, POLTH	Contains polar radius and angle for impact angle, amplitude and electrical distance of a ray impacting on receiving plane.
PSIL, PSIV	Difference is pointing error.
RECTX, RECTY	Information converted from polar information (POLR, POLTH) before summation.
RTEMP	Temporary storage for amplitude of ray segment just split from primary ray being followed; segment is RegionII reflection on bottom half of wedge and transmission segment to Region II on radome section in first quadrant.
SUMX(6), SUMY(6)	Sum for each slot of angle, amplitude and distance information for individual rays.
T2	Latest amplitude factor of primary ray being followed.

Variable List (continued)

UF2X0	Value of function representing the upper half (1st quadrant) of the inner surface (F2) at the point where the receiving plane (centered at $(X_o, 0)$) intersects.
VERTF1	X-coordinate of vertex of outer surface i.e. F1; Z-coordinate is zero.
VERTF2	X-coordinate of vertex of inner surface i.e. F2; Z-coordinate is zero.
XB, XC, XE	X-coordinates of points B, C, and E respectively; see diagrams.
XEM	X-coordinate of point where ray originates on emanating plane front.
XIM	X-coordinate of point where ray impacts on receiving plane.
XL, XV	Used for combining factors from rectangular sums: L for information from lower slots, (4th quadrant), U for information from upper slots (1st quadrant).
XLO	X-coordinate of point of intersection between receiving plane and lower part of F2 (4th quadrant).
XUP	X-coordinate of point of intersection between receiving plane and upper part of F2 (1st quadrant).
XX	Used in test of whether ray has crossed receiving plane (within Region III); contains XLO when ray is directed towards bottom and XUP when ray is directed towards top of radome.
YL, YU	See XL, XV
ZB, ZC, ZE	Z-coordinates of points B, C, and E respectively; see diagrams.
ZEM	Z-coordinate of point where ray originates, which is on emanating plane front.

Intermediate storage, which are variables, with no particular meaning are:
X, Y, S, U, LIM, CONST, and IT .

(6) Flow Chart - A Broad Outline of Logic Flow of FORTRAN Program

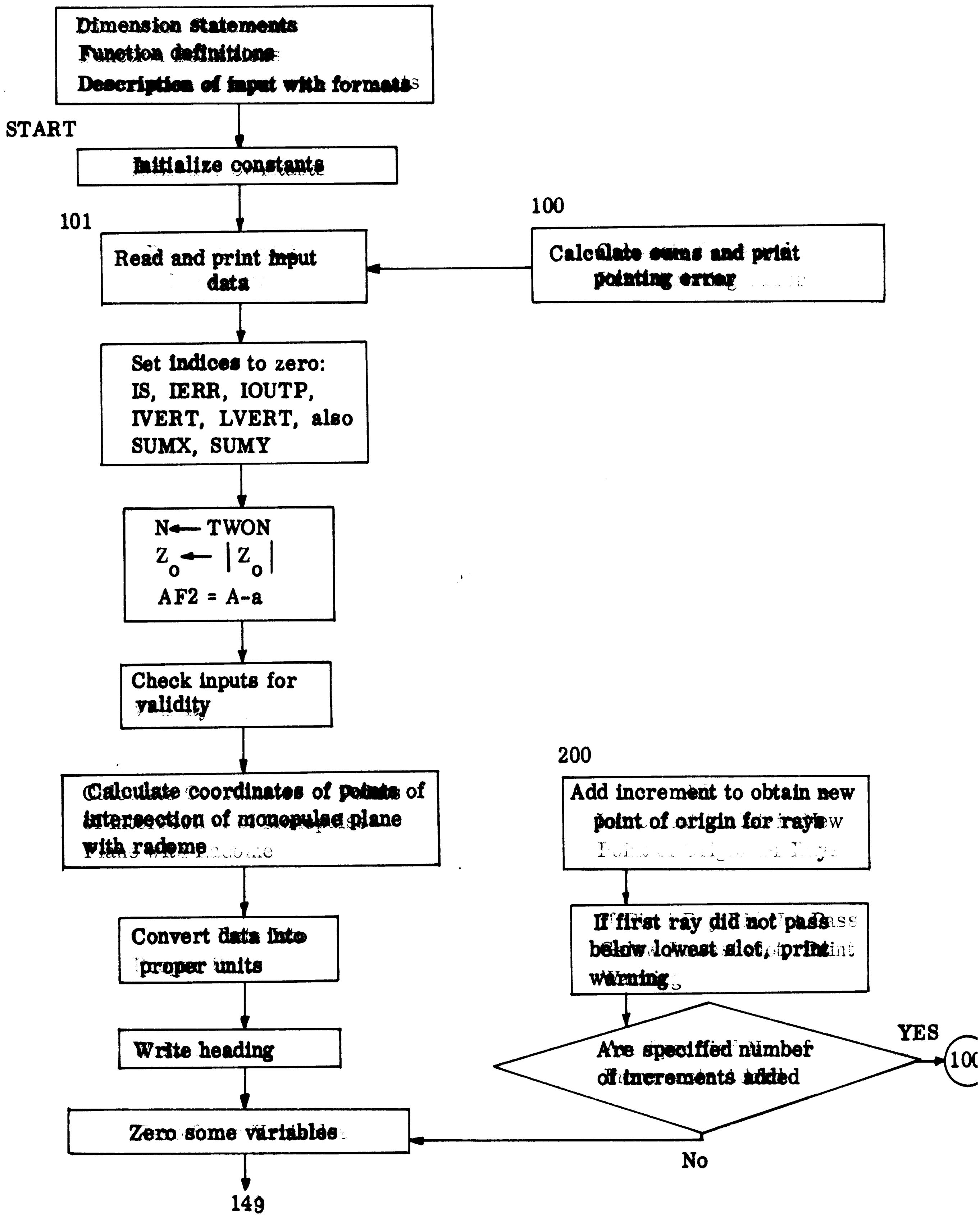

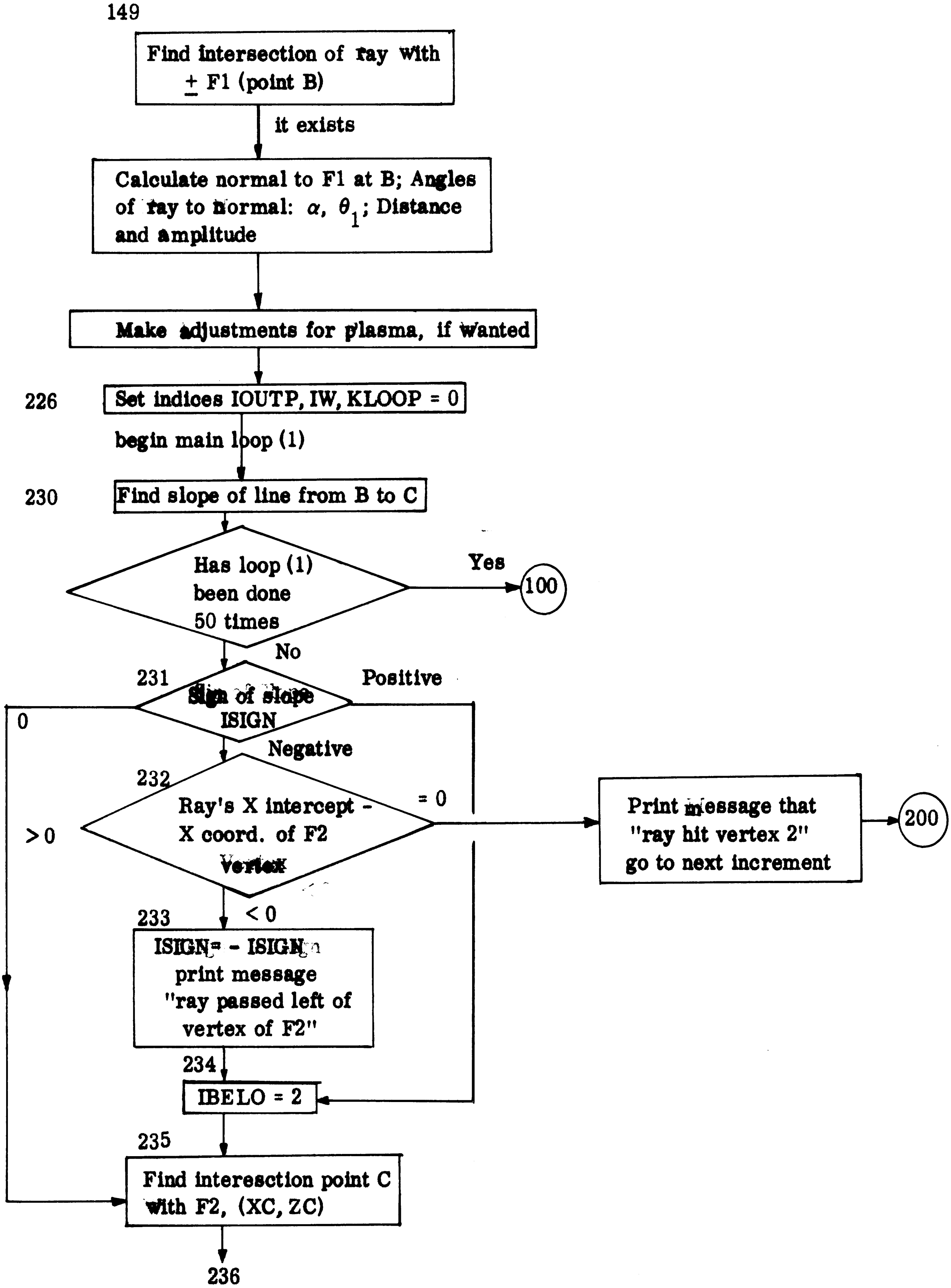
149
Find intersection of ray with ± F1 (point B)
it exists
Calculate normal to F1 at B; Angles of ray to normal: α, θ1; Distance and amplitude
Make adjustments for plasma, if wanted
226
Set indices IOUTP, IW, KLOOP = 0
begin main loop (1)
230
Find slope of line from B to C
Has loop (1) been done 50 times
Yes
100
No
231
Positive
Sign of slope ISIGN
0
Negative
232
Ray's X intercept - X coord. of F2 Vertex
= 0
Print message that "ray hit vertex 2" go to next increment
200
> 0
233
< 0
ISIGN = - ISIGN print message "ray passed left of vertex of F2"
234
IBELO = 2
235
Find interesction point C with F2, (XC, ZC)
236

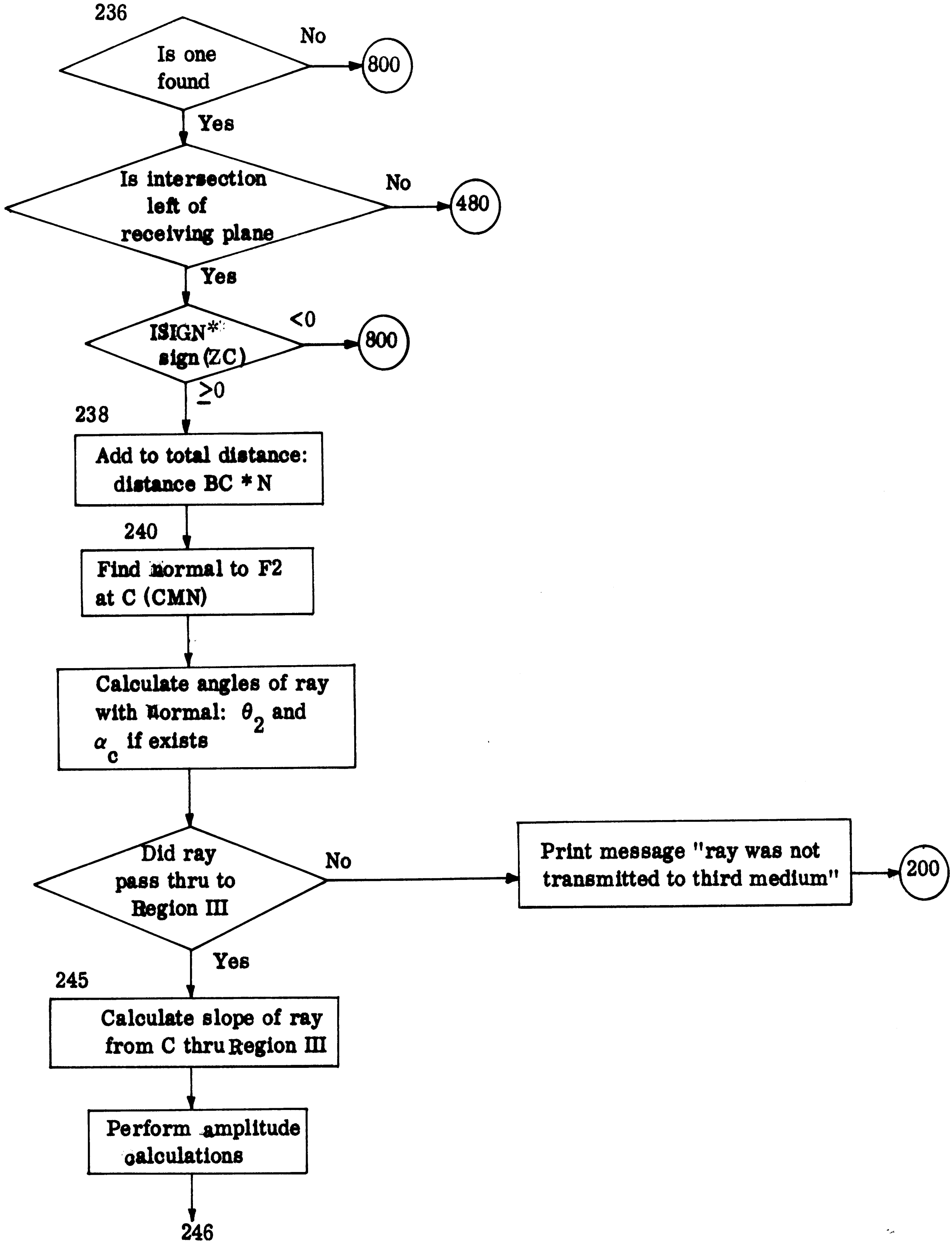
236
Is one found
No
800
Yes
Is intersection left of receiving plane
No
480
Yes
ISIGN* sign (ZC)
<0
800
≥0
238
Add to total distance: distance BC * N
240
Find normal to F2 at C (CMN)
Calculate angles of ray with normal: θ2 and αc if exists
Did ray pass thru to Region III
No
Print message "ray was not transmitted to third medium"
200
Yes
245
Calculate slope of ray from C thru Region III
Perform amplitude calculations
246

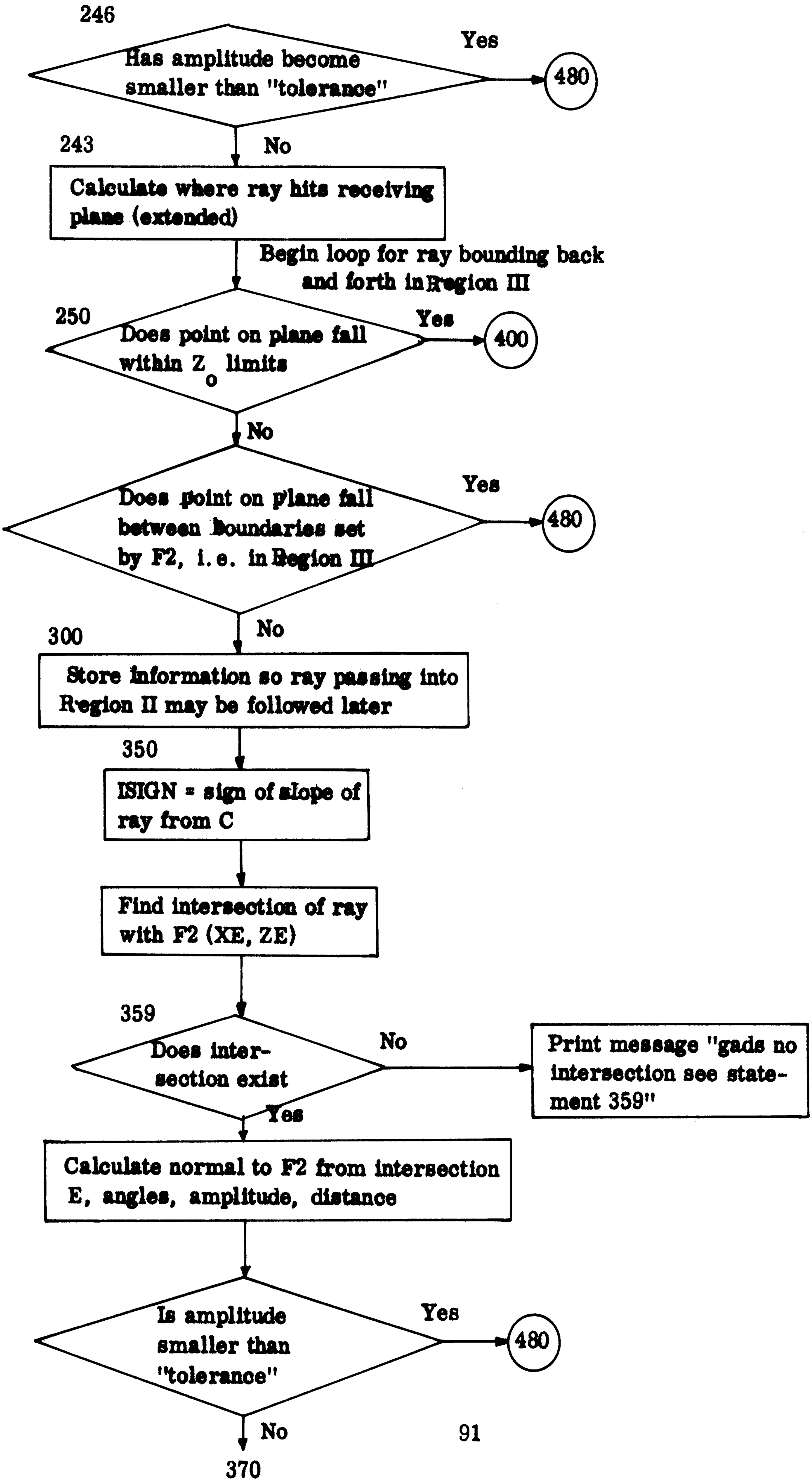
246
Has amplitude become smaller than "tolerance"
Yes
480
No
243
Calculate where ray hits receiving plane (extended)
Begin loop for ray bounding back and forth in Region III
250
Does point on plane fall within Z_o limits
Yes
400
No
Does point on plane fall between boundaries set by F2, i.e. in Region III
Yes
480
No
300
Store information so ray passing into Region II may be followed later
350
ISIGN = sign of slope of ray from C
Find intersection of ray with F2 (XE, ZE)
359
Does intersection exist
No
Print message "gads no intersection see statement 359"
Yes
Calculate normal to F2 from intersection E, angles, amplitude, distance
Is amplitude smaller than "tolerance"
Yes
480
No
370

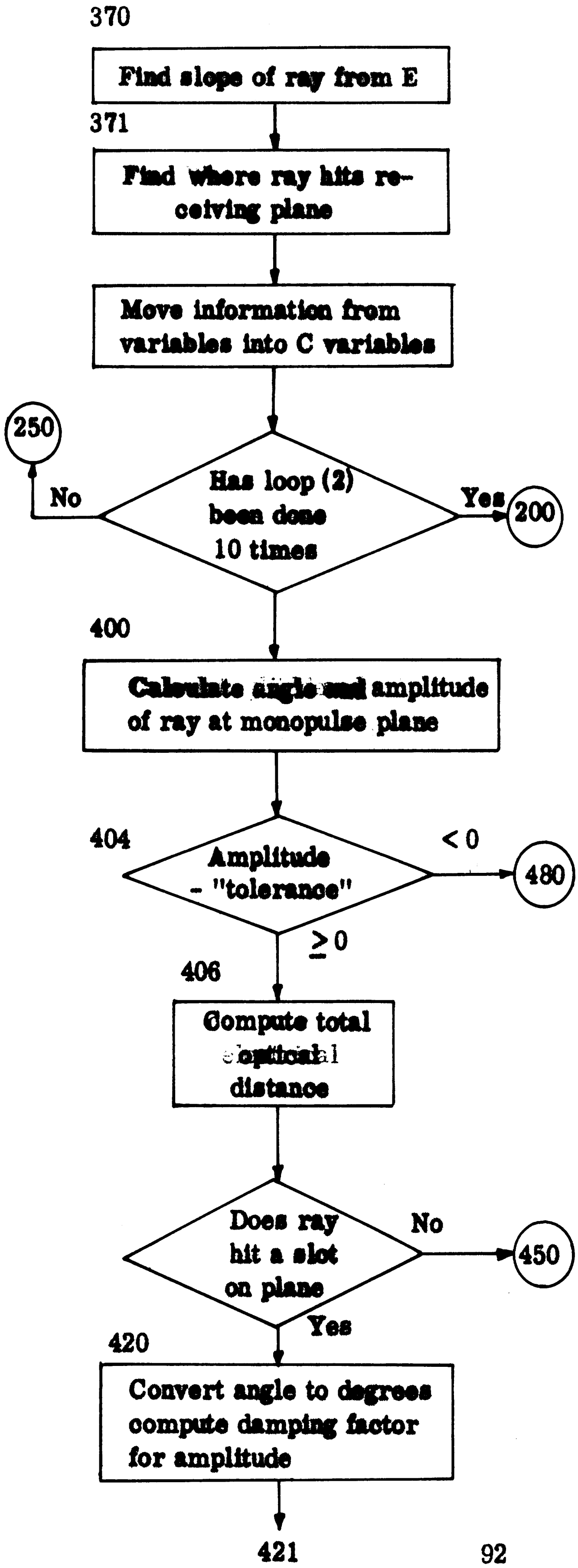
370
Find slope of ray from E
371
Find where ray hits re-ceiving plane
Move information from variables into C variables
250
No
Has loop (2) been done 10 times
Yes
200
400
Calculate angle and amplitude of ray at monopulse plane
404
Amplitude - "tolerance"
< 0
480
≥ 0
406
Compute total optical distance
Does ray hit a slot on plane
No
450
Yes
420
Convert angle to degrees compute damping factor for amplitude
421

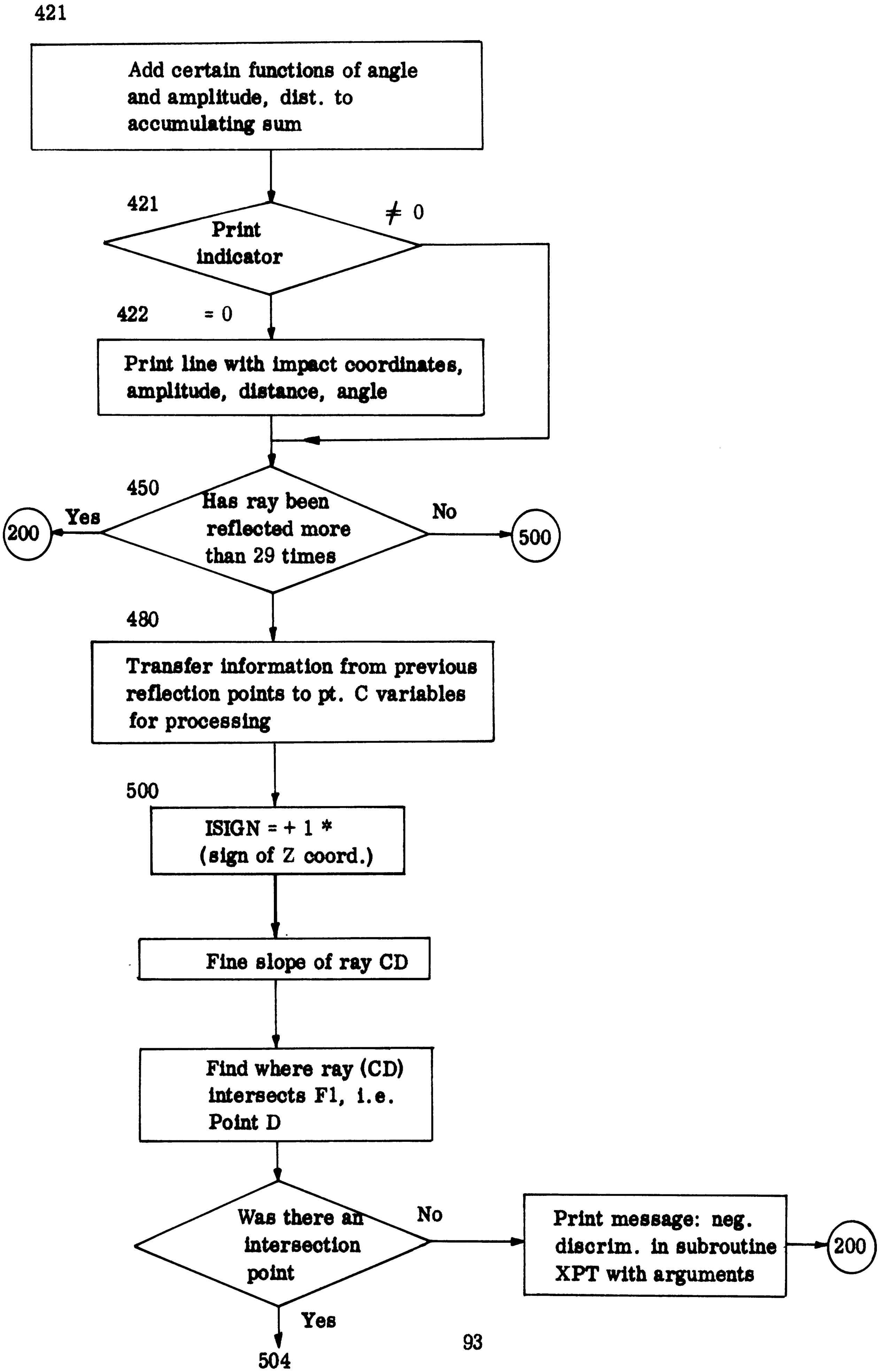
421
Add certain functions of angle and amplitude, dist. to accumulating sum
421
Print indicator
≠ 0
422
= 0
Print line with impact coordinates, amplitude, distance, angle
450
Has ray been reflected more than 29 times
Yes
200
No
500
480
Transfer information from previous reflection points to pt. C variables for processing
500
ISIGN = + 1 *
(sign of Z coord.)
Fine slope of ray CD
Find where ray (CD) intersects F1, i.e. Point D
Was there an intersection point
No
Print message: neg. discrim. in subroutine XPT with arguments
200
Yes
504

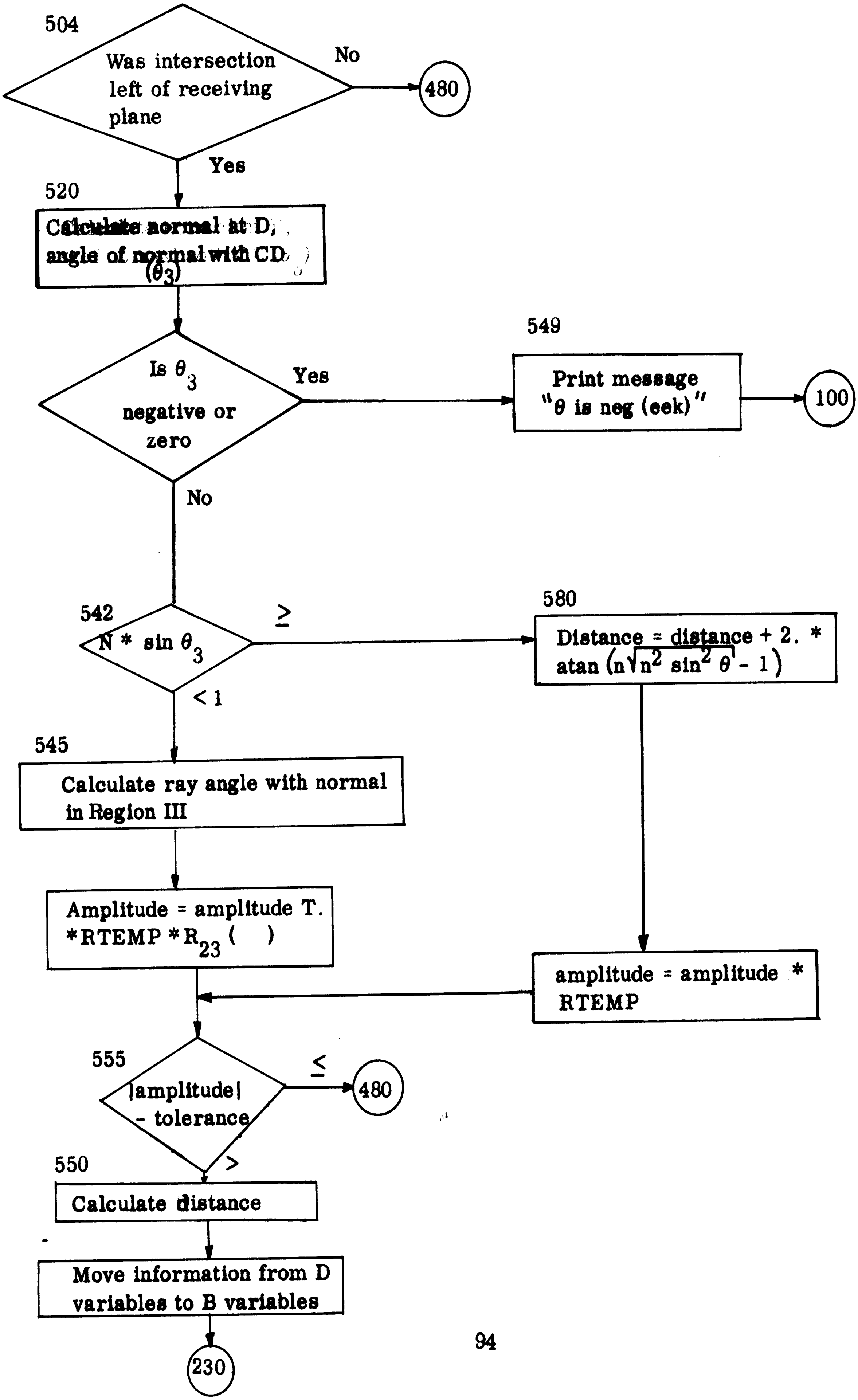
504
Was intersection left of receiving plane
No
480
Yes
520
Calculate normal at D, angle of normal with CD (θ_3)
549
Is θ_3 negative or zero
Yes
Print message "θ is neg (eek)"
100
No
542
N * sin θ_3
≥
580
Distance = distance + 2. * atan $(n\sqrt{n^2 \sin^2 \theta - 1})$
< 1
545
Calculate ray angle with normal in Region III
Amplitude = amplitude T. *RTEMP * R_{23} ( )
amplitude = amplitude * RTEMP
555
|amplitude| - tolerance
≤
480
>
550
Calculate distance
Move information from D variables to B variables
230

Then ray passes above +F2 or below -F2